SLAC-PUB-1533
January 1975

LARGE MOMENTUM TRANSFER PROCESSES*

R. Blankenbecler

Stanford Linear Accelerator Center
Stanford University, Stanford, California 94305

(Extracted from SLAC Summer Institute, SLAC Report 179, Volume I)

*Work supported by the U. S. Atomic Energy Commission.

I. INTRODUCTION

In these lectures we shall attempt to present an overall and hopefully unified description of large momentum transfer processes and the way in which it joins smoothly onto the familiar descriptions of the Regge and resonance regions at small momentum transfer. I shall try to give physically motivated arguments rather than mathematical detail. The theoretical picture that I shall utilize is the constituent interchange model, or CIM, developed by J. Gunion, S. Brodsky and myself.[1,2] Since we shall be dealing with a model, we must enumerate its ad hoc calculational rules and give either a theoretical or experimental motivation for them. The ultimate test of all recipes is the final result, however. The reason for introducing such ad hoc rules at this stage is two fold; it should allow us to relate quite different experimental results, and it should give us clues as to the ultimate underlying theory. We shall discuss strong interaction processes at two levels: the first is at an internal or basic level, in which possible internal structure of hadrons, constituents, binding forces, etc., are considered, and the second is at an external or hadronic level in which the emission on bremsstrahlung (both real and virtual) of hadrons is taken into account. In other words, the first level is the short range behavior and the second is the long range behavior of hadronic matter.

The first level will be called hadron irreducible since there are no extra inessential hadrons involved, and will yield dimensional counting rules[3] that simply state that the more constituents there are, the more "fragile" is the particle. We shall need to develop rules for calculating the behavior of generalized structure (or probability) functions and the fixed angle behavior of irreducible, basic processes.[4] Using these two results, we can then operate

at the hadronic level and join things together to make predictions about physical processes. If one is willing to assume arbitrarily the first two results, or to relate them in some way to form factor behavior, etc., then one need not ever work with constituents, and this is a very popular approach. The "soft gluon" model of Fried and Gaisser[5] is such an example, and while it is indeed different in detail from the CIM, these two pictures need not be fundamentally at odds with each other.

Let us consider, in transverse impact space, the collison of two composite hadrons. At large momentum transfer, the relevant impact parameters will be as small as possible and the finite sized hadrons will overlap in impact space. It is natural to expect then that an important force will be that between the constituents of one hadron and the containment field of the other hadron. This will naturally give rise to constituent interchange as a dominant force between hadrons in this large t region. Indeed, the CIM assumes that any other interaction can be neglected.

As the momentum transfer decreases, the collison will not necessarily be between the incident hadrons but can occur between secondaries emitted by them (which must then be reabsorbed on the way out after the collision in an exlcusive process). These secondaries will be predominantly hadrons since they are the lightest states and possess the longest compton wave lengths and have large coupling constants associated with their emission amplitude. Due to the finite size of the particles involved, these emissions and reabsorption processes occur at small average transverse momenta, and can become more and more important as the momentum transfer decreases. Furthermore, if the basic interchange process falls with increasing incident momenta, as most reasonable models suggest, then collisions between secondaries carrying only a small fraction of the incident momenta and hence small relative energy will dominate. This physical picture has therefore led us to a rather conventional explanation of the origin of Regge behavior in the subenergies--the interaction between

"wee" components of the incident particles to use Feynman's term. Furthermore, note that if more than one pair of secondaries interact, it will give rise to multiple exchange contributions, absorption effects with all the requisite nonplanar graphs, etc.

The advantage of this picture of the interaction is that it forces us to recognize that the Regge behavior in the forward direction must join smoothly and continuously onto the fixed angle behavior.[6] Since the backward Regge behavior must also join onto this same fixed angle behavior, there must also exist continuity relations between the forward Regge parameters and the backward Regge parameters. In practice, this leads to relations between the leading forward Regge trajectories and the leading backward Regge residues, and vice versa.[7]

II. MOTIVATION

One important empirical motivation for the CIM is the fact, which at SLAC is called the "J. Matthews theorem," that all meson-baryon cross sections are equal (more or less) at 90°. In Figs. 1, 2, 3, we see[8] that at 90° and $s \sim 10\ (\mathrm{GeV})^2$,

$$\frac{d\sigma}{dt}\,(M + B \to M' + B') \sim 0.1\mu b/(\mathrm{GeV}/c)^2$$

and also, for the <u>crossed</u> process $\bar{p}p \to \pi\pi$, one sees that

$$\frac{d\sigma}{dt}\,(\bar{p}p \to \pi\pi) \sim 0.05\mu b/(\mathrm{GeV}/c)^2 \ .$$

One simple way to interpret this remarkable fact is that if hadrons are composite objects, then once they are forced into a short enough range collision so that they overlap in impact space (by requiring a large angle scattering), then one simply has to rearrange the constituents and let the final particles emerge. If one rearranges the same number of constituents for all reactions, then the resultant cross sections should be roughly equal. Detailed calculations support this argument.

In addition, one should note that at 90°,

$$\frac{d\sigma}{dt}\,(pp \to pp)\Big/\frac{d\sigma}{dt}\,(\pi p \to \pi p) \sim 10^2$$

at 5 GeV/c. This means that nucleons must be coupled to the dominant short ranged force much more strongly than pions, because in this energy range, both theory and experiment suggest that pp scattering falls faster than πp scattering (s^{-10} vs. s^{-8}, respectively). This will be important to keep in mind when we try to pick out the most important graphs or subprocesses contributing to a particular reaction.

The CIM predicts that at fixed angle,

$$\frac{d\sigma}{dt} \sim \sum_i s^{-N_i}\, F_i(\theta) \ ,$$

where $N_0 < N_1 < N_2$, ... and hence as $s \to \infty$,

$$\frac{d\sigma(\theta)}{dt}\Big/\frac{d\sigma}{dt}\,(90°) \sim F_0(\theta)/F_0(90°) \ ,$$

and it is interesting to see if the data behaves this way. This ratio is shown for π^+p and K^+p elastic scattering[9] at 5 and 10 GeV/c in Fig. 4. The energy independence of $F_0(\theta)$ is consistent with this data. However, it would be nice to have such data on many more reactions and over a larger energy range. The interesting question is whether can we develop simple rules for computing the N_i and the $F_i(\theta)$. The neatest way to do this seems to be to assume a constituent model of the hadrons. This is the point where quarks enter our discussion, since to predict the angular distributions, quantum numbers must be assigned to the "point" constituents.

Our purpose here is to develop a description that works at large p_T but that also joins smoothly onto normal and familiar Regge behavior at small p_T. This is a non-trivial requirement for a theory, but it yields many

unexpected relations between a priori independent Regge parameters, and thereby many experimental checks.

III. KINEMATICS

For the most part, we shall be interested in describing exclusive and single particle inclusive reactions of the type

$$A + B \to C + D$$

and

$$A + B \to C + X ,$$

although we shall also briefly discuss correlations in inclusive reactions. For later purposes, it is convenient to define the momenta as

$$p_A = p + q + r$$
$$p_B = p$$
$$p_C = p + r$$
$$p_D = p + q$$

so that $s = (2p + q + r)^2$

$$t = q^2 \simeq -\frac{1}{2} s(1 - \cos\theta)$$
$$u = r^2 \simeq -\frac{1}{2} s(1 + \cos\theta)$$

and, of course, $s + t + u = M_A^2 + M_B^2 + M_C^2 + M_D^2$ for the exclusive case. However, for an inclusive reaction, one introduces the missing mass (squared) as

$$\mathcal{M}^2 = (p + q)^2$$

and the dimensionless ratio

$$\epsilon = \frac{\mathcal{M}^2}{s} \simeq 1 - \frac{|\vec{P}_C|}{|\vec{P}_C|_{max}} ,$$

where $|\vec{P}_C|$ is the magnitude of particle C's spatial momentum in the center of mass and finite particle masses have been neglected compared to s, t, u $\mathcal{M}^2$. It will prove convenient to define the transverse and longitudinal momentum fraction variables of particle C as

$$x_T = \frac{P_T}{|\vec{P}|_{max}} \simeq \frac{2P_T}{\sqrt{s}}$$

$$x_L = \frac{P_L}{|\vec{P}_C|_{max}} \simeq \frac{(t-u)}{s}$$

and then

$$\epsilon = 1 - (x_T^2 + x_L^2)^{1/2} .$$

These are easily described and visualized in the Peyrou plot shown in Fig. 5, where the x_T and x_L are fractional distances, and ϵ is the (fractional) distance to the boundary which corresponds to $\epsilon \to 0$ or exclusive scattering.

The reason for choosing the particle momenta as we have done is because in a particular class of frames, they have a simple parametrization.[6] This way of writing four-vectors we will call the <u>finite</u> momentum frame:

$$k = \left(xP + \frac{k^2 + \vec{k}_T^2}{4xP} , \vec{k}_T, xP - \frac{k^2 + \vec{k}_T^2}{4xP} \right) .$$

The parameter P is arbitrary (its value determines the frame) and one easily finds

$$\int d^4k = \int dk^2 \, d^2k_T \frac{dx}{2|x|} ,$$

to within delta functions arising from the Jacobian which usually don't contribute.

The usual infinite momentum frame variables are

$$k_+ = \frac{1}{2}(k_c + k_z) = xP$$

$$k_- = \frac{1}{2}(k_0 - k_z) = \frac{k^2 + k_T^2}{4xP} = \frac{M_r^2}{4k_+},$$

and the usual infinite momentum frame is the limit

$$k_3 = xP - \frac{k^2 + \vec{k}_T^2}{4xP} \longrightarrow \infty$$

$$k_0 = k_3 + \frac{k^2 + \vec{k}_T^2}{2xP} \longrightarrow k_3 + \frac{M_T^2}{2k_3} + \mathcal{O}(k_3^{-2})$$

In what we shall do here, this limit is not taken, and P is left arbitrary.

The four-momenta in the exclusive case can be shown to be (see all external masses equal for convenience)

$$p = \left(P + \frac{M^2}{4P}, \vec{0}_T, P - \frac{M^2}{4P}\right)$$

$$q = \left(\frac{q\cdot p}{2P}, \vec{q}_T, -\frac{q\cdot p}{2P}\right)$$

$$r = \left(\frac{r\cdot p}{2P}, \vec{r}_T, -\frac{r\cdot p}{2P}\right)$$

where $2q\cdot p = \vec{q}_T^{\,2}$, $2r\cdot p = \vec{r}_T^{\,2}$, and $\vec{q}_T\cdot\vec{r}_T = 0$. The same basic parametrization will be used in the inclusive case, but, of course, since $\mathcal{M}^2$ is arbitrary, the subsidiary conditions on the vectors q and r are modified.

IV. DIMENSIONAL COUNTING RULES

One of the more important recent developments in dyanmics has been the formulation of the dimensional counting rules by Brodsky and Farrar.[3] These rules allow one to quickly estimate the behavior of exclusive and inclusive reactions, form factors, structure functions, etc., at large momentum transfers. These rules have not been derived rigorously, indeed there are some exceptions to them in certain theories and certain reactions, but in the type of model of hadrons that we need to describe the present data, they seem to be consistent with both theory and experiment.

These rules will predict, in agreement with our intuition, that the more constituents that are involved in a coherent fashion, the faster the fall off of the matrix element at large values of all kinematic variables. This means that the simplest configuration in bound states with the minimum number of constituents will contribute the leading terms. Now the pion wave function, in the quark model for example, surely involves a sum over arbitrary numbers of quark paris, but at large angles, only the single $(\bar{q}q)$ configuration contributes to the leading behavior.

A. Form Factors

The two particle bound state wave function will be described by a covariant wave function with particle of momenta k and $p-k$ as shown in Fig. 6a, with p and k written using the finite momentum variables x, $\vec{k}_T$, k^2, and P as described earlier. Consider first the matrix element of a single particle operator Q_q, such as the current operator, which brings a momentum transfer q into the system. We will ignore the algebraic complication due to spin and discuss only spin zero constituents. The quality of interest in the large q^2 behavior of the matrix element

$$M(q^2) = \langle p + q|Q_q|p\rangle$$

which is illustrated in Fig. 6b. The states are wave functions and the operator Q_q contains the requisite spectator particle propagators G_i, such as, for example, $Q_Q = j_1 G_2^{-1}$. Now the wave functions will satisfy a Bethe-Salpeter type of equation with an interaction kernel K, where

$$\langle p| = \langle p|\, KG_1G_2.$$

Using this result into the matrix element M allows it to be written in terms of a "well-tempered" operator $\bar{Q}_q$, where

$$\bar{Q}_q = KG_1G_2Q_q = Q_qG_1G_2K \ .$$

$\bar{Q}_q$ is a connected operator with the same matrix elements in the bound state as Q_q. It has the advantage that since it treats all the particles in the bound state on the same footing, it is straightforward to estimate its magnitude, especially for large q^2.

Choosing the interaction between the constituents to be <u>renormalizable</u>, such as $\lambda\varphi^4$, or a vector gluon theory, the lowest order term in K is a constant at large momentum transfer (fixed angle scattering). Using Fig. 7a, which illustrates the momentum flow in $\bar{Q}_q$ and the two regions that contribute to the final result, the matrix element defining the form factor is

$$M = \iint \psi(y,k',p+q)\ \lambda\ \frac{\epsilon\cdot(2k+q)}{(M^2-(k+q)^2)}\ \psi(x,\ k,\ p+q)\ .$$

Using $(k+q)^2 = q^2(1-x) + O(k)$, and assuming that the wave functions fall sufficiently fast so that all components of k are finite, the form factor F and the matrix element become

$$M = \epsilon(2p+q)\ F_2(q^2)$$

where

$$F_2(q^2) \cong \frac{\lambda}{q^2}\ \langle\frac{x}{1-x}\rangle\ [\int \psi\ d^4k]^2$$

and $\langle\rangle$ means average value in the bound state. This now leads us to the next fundamental assumption that the above averages and integers $\int \psi\ d^4k = \psi(x_\mu = 0)$ are finite, hence $F_2 \sim \lambda(\vec{q}_T^{\,2})^{-1}$. If there is a divergence, then one has to go back and carry out a more careful estimate of the q^2 behavior. Logarithmic modifications are probably to be expected and can arise from the $(1-x)$ factor.

The three particle bound state can be treated in the same fashion. Referring to Fig. 7b, we see immediately that the bound state equation must be iterated twice in order to spread the momentum transfer q among the final particles. The three particle form factor F_3 will then fall as

$$F_3(q^2) \sim \lambda^2(\vec{q}_T^{\,2})^{-2}\ .$$

The behavior of F_3 has been discussed carefully and in detail by C. Alabiso and G. Schierholtz who used a relativistic bound state equation and included the effects of spin. They discuss the general case and agree with the above in the limit of a renormalizable interaction.

In an N-particle bound state, an obvious extension of the previous discussion yields the result

$$F_N \sim \lambda^{N-1}(\vec{q}_T^{\,2})^{1-N}\ .$$

The above discussion assumed that the interaction between the constituents was of a renormalizable type. A super-renormalizable interaction yields a different result. For example, a $(\nu\varphi^2\chi)$ theory produces a kernel K that falls as ν^2/t, and the two particle form factor then behaves as $\nu^2(\vec{q}_T^{\,2})^{-2}$.

The present data is not very decisive, but $e^+e^- \to \pi^+\pi^-$ data suggests that the pion form factor behaves as a monopole and hence that the appropriate model of the pion is a $(\bar{q}q)$ bound state, with the q's interacting via a renormalizable interactions.

The present data for the nucleon form factor is consistent with a dipole falloff and hence there are <u>two</u> possible models for the baryons:

(1) B = (3q), interacting via a renormalizable interaction.

(2) B = (q + "core"), interacting via a super-renormalizable interaction.

The first model obeys the simple dimensional counting rules and will be used throughout these lectures for simplicity. The second model is consistent with most of the data and has some virtues. However, one cannot choose between them at the moment on the basis of the large t data. The second model is the one used in our first papers on the CIM, and it will be referred to occasionally during our discussion. It has several interesting theoretical features and experimental advantages.

B. Scattering Amplitudes

The limiting behavior of scattering amplitudes at fixed angle can be handled by the same type of argument. The basic problem is to iterate the bound state equations so that the large momenta (q and r) are evenly distributed among the final particles so that they can bind. Consider a pion-pion scattering graph as depicted in Figs. 8a and 8b. If the vector k is parametrized in terms of x, k_r and k^2 as before, the invariant scattering amplitude can be easily estimated after iterating K three times as

$$M_a \sim \frac{\lambda^2}{q_T^2 r_T^2} \left\langle \frac{1}{x(1-x)} \right\rangle \psi_n^4(0)$$

$$M_a \sim s^{-2} f_2(\theta) .$$

The diagram in Fig. 8b is given directly in terms of the pion form factor as

$$M_b = \lambda F_n^2(t) \sim s^{-2} f_b(\theta)$$

It is seen that the exchange graphs of the form given by Fig. 8a, and the terms which can be obtained by permutation of p_A, p_B, p_C and p_D all fall with the same rate as the more familiar gluon exchange diagrams. While the contributions M_a and M_b both fall as s^{-2}, they have a quite different angular dependence. The resulting differential cross section a fixed angle falls as $d\sigma/dt \sim s^{-2}|M^2| \sim s^{-6}$.

The scattering of a two body (pion) state off of a three body (baryon) state can be handled in the same fashion. Using the momenta as shown in Fig. 8c, and describing k' in terms of x', k_T', and k'^2, this diagram behaves as

$$M_c \sim \frac{\lambda^4}{r_T^2 (q_T^2)^2} \left\langle \frac{1}{x(1-x)(1-x')} \right\rangle \left\langle \frac{1}{1-x} \right\rangle \psi_n^2(0)\, \psi_B^2(0,0)$$

$$\sim s^{-3} f_c(\theta)$$

and hence $d\sigma/dt \sim s^{-8}$. A similar treatment of a three body state off a three body state can be carried out in a similar fashion and one finds that $d\sigma/dt \sim s^{-10}$. In general, one can show by induction that

$$\frac{d\sigma}{dt} \sim s^{2-N_{tot}} f_{ABCD}(\theta) ,$$

where

$$N_{tot} = n_A + n_B + n_C + n_D .$$

This is a general result and will be useful in all our subsequent discussion.

It should be pointed out that if the nucleon is a (q + "core"), then the pion-proton cross section falls as s^{-8} which is the same as the (3q) case. However, the proton-proton cross falls as s^{-12} rather than s^{-10} as in the (3q) model.

In the following table, the predictions for some selected processes are given together with the experimental values of the s falloff where it is known with sufficient accuracy.

TABLE 1

Process	$d\sigma/dt$	exp. power
$\gamma p \to \gamma p$	s^{-6}	
$\gamma p \to \pi p$	s^{-7}	7.3 ± 0.4
$\to \pi\Delta$	s^{-7}	$\sim 7\text{-}8$
$\pi p \to \pi p$	s^{-8}	7.7 ± 0.6 $(\bar{\pi}p \to \bar{\pi}p)$
$\to \pi\Delta^*$	s^{-8}	9.3 ± 0.5 (CEX)
$\to \rho p$	s^{-8}	
$\bar{p}p \to \pi\pi$	s^{-8}	
$pp \to pp$	s^{-10} or s^{-12}	10 ± 0.7
$\to pN^*$	s^{-10} or s^{-12}	$10 \sim 12$
$\bar{p}p \to \bar{p}p$	s^{-10} or s^{-12}	?

C. Limiting Regge Behavior

A full theory, or a complete model, should determine the angular behavior $f(\theta)$ as well as the power of s. It must be able to separate behaviors in s from t from u. It will be shown later that the graphs that involve interaction between constituents in different hadrons such as in Fig. 8b do not seem to contribute significantly to the experimental cross sections. If these graphs are discarded, then the variables can be separated by a more careful graphical analysis[4] and one finds that for fixed t, as $s \simeq -u$ gets large, scattering amplitudes approach the form (only dominant graphs are considered)

$$M \sim s^{\alpha_{AC}(-\infty)} \beta_{BD}(t) + \cdots$$

where

$$\alpha_{AC}(-\infty) = \frac{1}{2}(4 - n_A - n_B - n_I)$$

$$\beta_{BD}(t) \sim (-t)^b, \qquad b \equiv \frac{1}{2}(n_I - n_B - n_D)$$

and n_I is the number of constituents exchanged in the t channel. Examples of this predicted behavior are (all are evaluated at $t = -\infty$):

$\alpha_{nn} = -1$	$I = 0$ and 1
$\alpha_{pp} = -2$	$I = 0$ and 1
$\alpha_{\bar{p}p} = -4$	exotic
$\alpha_{\pi^+\pi^-} = -2$	double CEX
$\alpha_{\pi p} = -2$	baryon, Δ exchange
$\alpha_{\gamma\gamma} = 0$	$J = 0$ fixed pole
$\alpha_{\gamma\pi} = -1/2$	
$\alpha_{\gamma p} = -3/2$	

In the original CIM model of the baryon as a (q + "core"), the pp trajectory has the limiting value $\alpha_{pp}(-\infty) = -3$. The effective trajectory for pp scattering is shown in Fig. 9 and for $\pi^- p$ scattering in Fig. 10. Even though the errors are large, the trend is apparent.

An interesting application of the above formulae is to large angle and backward $\bar{p}p$ scattering. Backward scattering should be described by double baryon exchange which is predicted to behave as $\alpha_{\bar{p}p}(-\infty) = -4$, and $b = 0$. Since $\alpha_{\bar{p}p}$ is an exotic channel, it is natural to assume that it does not rise very far above its asymptotic value even at $t \simeq 0$. If $\alpha_{\bar{p}p}(t) \simeq -4$ for all $t < 0$, then one predicts $d\sigma/dt \sim s^{-10}$ in the entire large angle and backward regions. This behavior is entirely consistent with the deuteron lying at $t \simeq 4M^2$ on this trajectory.

D. *Distribution Functions*

The second fundamental result that we shall need, besides the fixed angle behavior, is the threshold behavior of the particle distribution functions which are simply related to what might be called generalized structure functions. We shall define $G_{H/A}(z)$ to be the probability of finding an (off-shell) particle H in the momenta (defined in the usual finite momentum frame). Now momentum conservation is expressible as

$$\sum_H \int dz\, z\, G_{H/A}(z) = 1$$

and the deep inelastic structure functions are expressible as

$$F_{2A}(x) = x \sum_q \lambda_q^2\, G_{q/A}(x)$$

where λ_q is the charge of the quark of type q.

A quark q can arise directly from the guts of particle A (which will be called hadron irreducible) or from a secondary hadron H which has been emitted by A (this will be called hadron reducible). Therefore, one clearly has the formula corresponding to these words

$$G_{q/A}(x) = \int_x^1 \frac{dz}{z} \sum_H G^I_{q/H}(x/z)\, G_{H/A}(z) ,$$

where the superscript I means hadron irreducible, and serves to avoid possible double counting. The full deep inelastic structure function can be written using this decomposition in the transparent form

$$F_{2A}(x) = \int_x^1 \sum_H F^I_{2H}(x/z)\, G_{H/A}(z) .$$

These formulae require that the probability function contain a delta function, i.e. $G_{A/A} \sim \delta(1-z)$.

Using an extension of the arguments used previously in our discussion of the dimensional counting rules, the threshold behavior $(x \sim 1)$ is found to be (see Refs. 4 and 10 for details)

$$G_{q/B}(x) \sim G^I_{q/B}(x) \sim (1-x)^{g(q/B)}$$

where

$$g(q/B) = 2n(\bar{q}B) - 1$$

and $n(\bar{q}B)$ is the minimum number of quarks in the state $(\bar{q}B)$, and, of course, $1 + n(\bar{q}B)$ is the minimum number of quarks in the state B. This is consistent with the Drell-Yan-West relation, since the form factor of B behaves as $F_B \sim (\sim q^2)^{-n(\bar{q}B)}$.

Using the above equations, the only consistent threshold behavior of the probability functions for finding hadron H in hadron B is

$$G_{H/B}(z) \sim (1-z)^{g(H/B)}$$

where

$$g(H/B) = 2n(\bar{H}A) - 1$$

and $n(\bar{H}B)$ is the minimum number of quarks in the hadronic state $(\bar{H}B)$. This remarkable result depends on the assumption of an underlying scale invariant theory at the constituent level and on the number of constituents.

Some typical values of $g(H/B)$ which will be useful later are the familiar results for quark $g(q/\pi) = g(\bar{q}/\pi) = 1$, $g(q/P) = 3$, $g(\bar{q}/P) = 7$, and the new results for hadrons, $g(B/B) = -1$ or 3, $g(\pi/p) = 5$, $g(K^+/p) = 5$, $g(K^-/p) = 9$, and $g(\bar{p}/p) = 11$. The value $g(B/B) = -1$, actually corresponds to the $\delta(1-z)$ term that is present in $G_{B/B}$. The physical interpretation of the systematics of these results is clear--the rate of vanishing of G depends on the number of degrees of freedom of the debris left behind (near the threshold) in producing the leading particle H. The number $n(\bar{H}B)$ is the number of constituents that must be stopped if H is to have x near 1.

The Regge behavior of the probability functions shows up in the power behavior for small z, i.e. $G \sim z^{-\alpha(0)}$. Throughout our discussion we shall therefore set

$$G_{H/A}(z) = z^{-\alpha_A(0)}(1-z)^{g(H/A)} ,$$

where $\alpha_A(0) = 1$ (Pomeron), but this could be multiplied by any smooth function of z (better data will certainly require this modification) without affecting our results on the general behavior of amplitudes.

E. Hadron Decays

The probability function $G_{H/A}(z)$ describes the fractional longitudinal momentum distribution which is perhaps most easily interpreted in the infinite momentum frame of A. It is possible, however, to determine some interesting properties of G by measurements in a general frame, including the rest frame of A. This may be very interesting in relating the decays of system with a large Q value, such as annihilation processes, and the decay of coherent states produced by diffractive excitation reactions.[4] Consider the decay $A \to a + X$ in the rest frame of A and the rate

$$\frac{d\Gamma}{d\omega} \equiv d_{a/A}(\omega), \qquad \omega = \frac{2E_a}{M_A} .$$

The decay can also be described in terms of the infinite momentum frame variable $x = (E_a + k_a^z)/M$, which leads to the spectrum

$$\frac{d\Gamma}{dx} \equiv D_{a/A}(x) = \int_0^1 d\omega \left[\omega^2 - \frac{4a^2}{M_A^2}\right]^{-1/2} d_{a/A}(\omega)\ \theta\ \omega\left[- x - \frac{a^2}{M_A^2 x}\right]$$

Now it has been shown in a quite general model (and it is what one would expect) that if $G_{a/A}(x) \sim (1-x)^g$, then $D_{a/A} \sim (1-x)^g$. Therefore as $\omega \sim 1$

$$d_{a/A}(\omega) \simeq (1-x)^{g(a/A)^{-1}}$$

The example of $(\bar{N}N)$ annihilation into a leading pion has been analyzed by Pelaquier[11] and the data seems to be consistent with the prediction $g(\pi/\bar{N}N) = 3$. Many other examples need to be analyzed and their threshold behavior extracted, especially excitation reactions. The familiar parton prediction

$$d_{\pi/(e^+e^-)} \sim (1-\omega)$$

follows after the photon spin is taken into account.

F. Angular Distribution

While the dimensional counting rule giving the energy falloff depends on the inter-constituent force and their number, the expected angular distributions depend on the quantum numbers of the constituents. For example, if the incident hadrons can exchange constituents and produce the final state, then this (ut) contribution illustrated in Fig. 11a will yield an amplitude of the general form $M_a \sim (-u)^{-A}(-t)^{-B}$, which produces an angular distribution characterized by a forward and backward peak.

If antiparticles are present, such as in pion-nucleon scattering, the (st) contribution of Fig. 11b will produce only a forward peak. The gluon exchange process of Fig. 11c will produce a forward peak only, and $M_c \sim (-t)^{-B}$ or $s(-t)^{-B}$ for a spin zero and spin one gluon respectively. In both cases, this term produces a high effective trajectory value and essential equality of particle-particle and particle-antiparticle scattering. Both of these behaviors are in disagreement with the present data and its trends. This is the reason why it was necessary to exclude these types of diagrams from the original CIM. As we shall see, this exclusion rule allowed a correct prediction of the large p_T behavior subsequently found in the ISR data.

Since there are no antiquarks present in the lowest configuration in the proton's wave function, only the (ut) term can contribute to pp

scattering (also true for K^+p) and one expects that for finite t,

$$s^2 \frac{d\sigma}{dt}(pp) \sim (-u)^{2\alpha(t)} \beta^2(t) ,$$

where $\alpha(t)$ is an effective trajectory and $\alpha(-\infty) = -2$ (or -3 in (q + "core") model). From crossing, only the (st) term can contribute to $\bar{p}p$ scattering (and K^-p)

$$s^2 \frac{d\sigma}{dt}(\bar{p}p) \sim (s)^{2\alpha(t)} \beta^2(t)$$

and hence

$$R(\theta) = \frac{d\sigma(pp)}{d\sigma(\bar{p}p)} \sim \left(\frac{s}{-u}\right)^{-2\alpha(t)} \sim \left(\frac{2}{1 + \cos\theta}\right)^{-2\alpha(t)}$$

Thus a characteristic difference in angular distributions is expected in the model, and furthermore, $R(90°) \sim 2^4$ or 2^6, depending on the nucleon model assumed ($\alpha = -2$ or -3 respectively).

Predictions for the angular distribution of the processes $\pi^\pm p \to \pi^\pm p$, $K^\pm p \to K^\pm p$, $\pi^- p \to \pi^0 n$, and $K_L p \to K_S p$ are in reasonable agreement with the data.[12]

V. BASIC PROCESSES

The CIM model for inclusive and exclusive reactions begins with a basic irreducible process and then adds on the possibility of hadronic bremsstrahlung to "dress" and Reggeize the process. As the transverse momentum in the overall process of interest increases, the bremsstrahlung is suppressed and the basic process will dominate the reaction. Consider the irreducible contribution to elastic scattering illustrated in Fig. 12a, in which the projectile A scatters from a constituent q in the target particle B. The differential cross section can be written in the obvious form

$$\frac{d\sigma}{dt} \sim \sum_q (F^q_{BD}(t))^2 \frac{d\sigma}{dt}(A + q \to C + q)\Big|_{\substack{s'=\langle x\rangle s \\ t'=t}}$$

where the cross section for $A + q \to C + q$ is evaluated at an averaged reduced energy because constituent q is carrying only a fraction x of the momenta of the state B. The function $F^q_{BD}(t)$ is a "form factor" whose asymptotic dependence can be computed using the dimensional counting rules.

Now consider the inclusive reaction $A + B \to C + X$ at a missing $(\text{mass})^2$ of $\mathcal{M}^2$. Again one of the basic scattering processes is $A + q \to C + q$ is shown in Fig. 12b, and the generalized structure functions of the target B obviously come in to the amplitude. One finds after an elementary calculation

$$E\frac{d\sigma}{d^3p} = \sum_q \frac{s}{\pi(s+u)} x\, G_{q/B}(x) \frac{d\sigma}{dt}(A + q \to C + q)\Big|_{\substack{s'=xs \\ u'=xu \\ t'=t}} ,$$

where $x \equiv -t/(s + u) = -t/(\mathcal{M}^2 - t)$, ($x$ is the familiar Bjorken scaling variable). If particles A and C were electrons, this reduces to the usual scattering answer and since a factor of the $(\text{charge})^2$ of the constituent factors out of each of the basic cross sections, the sum over q then leads to the E and M structure function:

$$E\frac{d\sigma}{d^3p} = \frac{s}{\pi(s+u)} F_{2B}(x) \frac{d\sigma}{dt}(e + q \to e' + q')\Big|_{\substack{s'=xs \\ t'=t}} .$$

Since there is a relation between the probability functions G and the form factors F expressed by the Drell-Yan-West relation,[13] one might expect that there will be a relation connecting the inclusive and exclusive cross sections for small missing mass. In the resonance region for electroproduction, a relation has been found and is called Bloom-Gilman duality.[14] A similar sort of relation might be expected to hold in the hadronic case, and it does.[15]

For small missing mass, x approaches unity since $x = 1 - \mathcal{M}^2/(\mathcal{M}^2 - t)$. The probability functions G vanish as a calculable power given by dimensional counting. Using the relation

$$\frac{d^2\sigma}{dt\, d\mathcal{M}^2} = \frac{\pi}{s} E \frac{d\sigma}{d^3p} ,$$

the cross section into a differential mass bin at $\mathcal{M}^2$ is proportional to

$$\frac{d^2\sigma}{dt} \propto \frac{d\mathcal{M}^2}{\mathcal{M}^2} \left[\frac{\mathcal{M}^2}{\mathcal{M}^2 - t}\right]^{g(q/B)+1} \frac{d\sigma}{dt}(A + q \to C + q)\Bigg|_{\substack{s'=s \\ u'=u \\ t'=t}} ,$$

and one recognizes that the large t dependence is the same as for elastic scattering since

$$\left[\frac{\mathcal{M}^2}{\mathcal{M}^2 - t}\right]^{g(q/B)+1} \simeq (F^q_{BD}(t))^2 .$$

These two processes therefore have the same behavior on the kinematic variables in this limit but unfortunately a calculation of the relative normalization is difficult. One of the difficulties is the fact that at small missing mass, many of the final states in inclusive scattering become coherent so that one cannot just perform the incoherent sum over them as in the above formulas which hold at larger missing mass. In any case, we see that there is a smooth connection between inclusive and exclusive processes both at fixed $|t|$ and at fixed scattering angle.

VI. REGGE BEHAVIOR

We have seen that the typical basic scattering process between hadrons falls with energy at fixed angle rather rapidly in the CIM. This is true even at fixed momentum transfer unless there is a direct vector gluon force (which we have argued must be negligible). The basic scattering process can be considered as in Fig. 13a. If it falls as s increases at fixed t, then the system will prefer to scatter through diagrams of the form shown in Fig. 13b. In this virtual bremmstrahlung diagram, particle A converts to H with a fraction x of the incident momentum and other coherent "stuff" with momentum $(1-x)$. The basic process is thereby converted to $H + B \to H' + D$ scattering at the reduced effective energy $s' \simeq xs$. If x can be small, then this process is not suppressed much if H' can pick up the momentum fraction $(1-x)$ and convert to C. This latter process is suppressed as t increases, so that in the large t and eventual fixed angle limit, the irreducible process (Fig. 13a) will dominate. This is the physical origin of Regge behavior in this model at small t. It is dominated by the emission and absorption of the less massive hadronic states. They therefore control the long distance or small t behavior of the amplitudes.

The above discussion can be made more precise[6] and one finds that such graphs produce a Regge trajectory of the form

$$\alpha(t) = \alpha(-\infty) + A(t) ,$$

where $A(t)$ vanishes in a calculable way as $|t|$ increases (the power can be calculated by dimensional counting). A similar result holds for the residue function. This behavior assures that the fixed angle behavior joins smoothly to the Regge behavior.

However, one should note that the earlier predictions were $\alpha_{\pi p}(-\infty) = -1$, and $\alpha_{pp}(-\infty) = -2$. Since factorization should hold, how can this behavior be tolerated? Fortunately, the equations are very clever and make these behaviors consistent in the simplest way possible. When one treats the coupled channel system (which must be done in order to check factorization) of $\pi\pi \leftrightarrow \bar{p}p$ in the t-channel, one finds that there must be at least 3 important trajectories which are related.

The matrix elements for $\pi\pi$, πp, and pp scattering must have the form (neglect signature here)

$$M = \beta_+(t)(-u)^{\alpha_+(t)} + \beta_-(t)(-u)^{\alpha_-(t)} + \beta_0(t)(-u)^{\alpha_0(t)} + \cdots$$

where $\alpha_+(-\infty) = \alpha_-(-\infty) = -1$, and $\alpha_0(-\infty) = -2$ (or -3). For $\pi\pi$ and πp scattering, there is no particular relation between the residues. However, in the pp case, one finds that at large t, $\beta_+(t) = -\beta_-(t)$ and the first two terms cancel, leaving a residue which is smaller than the third term which then produces the expected fixed angle behavior.

The theoretical calculation leads one to expect that $\alpha_+(t)$ rises at small t and should be identified with the familiar Regge trajectories there. However, α_- should deviate only slightly from its asymptotic value (probably below it). It was predicted in Ref. 6 that when $\alpha_+(t)$ drops to ~ -1, the first two terms should cancel and the fixed angle result should hold. Since $\alpha_+(t)$ should control πp scattering, the effective trajectory behavior shown in Fig. 11 leads us to expect that for $|t| > 2$ or 3, the fixed angle result should hold. For somewhat smaller $|t|$, one expects the power behavior to be more like that found in πp scattering. These predictions seem to be in rough agreement with the data but a more extensive analysis is clearly needed to see if this cancellation mechanism is occurring. If cuts become important, which may well be the case in pp scattering at ISR energies, the effective trajectory will drop even slower to its asymptotic value.

VII. TRIPLE REGGE REGION

Let us reexamine the inclusive formula given in Section V by including the Regge effects just discussed. The contribution from a single particle q is of the form

$$E\frac{d\sigma^q}{d^3p} = \frac{s}{\pi(s+u)}\, xG_{q/B}(x)\, \frac{d\sigma}{dt}\,(A + q + C + q)\Big|_{\substack{s'=xs\\ u'=xu\\ t'=t}}$$

where in light of our Regge analysis we now have

$$\frac{d\sigma}{dt}\,(A + q \to C + q) = \left|\gamma(t')(-u')^{\alpha_{AC}(t')} + \tilde{\gamma}(t')(-u)^{\alpha_{AC}(t')}\right|^2 / s'^2$$

and $\gamma(-\infty) = \text{constant}$. Retaining only the γ-term for simplicity (one needs both terms to get the angular distribution correct), the inclusive cross section achieves the form $(\alpha_B(0) = 1)$.

$$E\frac{d\sigma^q}{d^3p} = \left(-\frac{u}{s}\right)^2 \frac{\gamma^2(t)}{(p_T^2 + M^2)}\, xG_{q/B}(x) \left[\frac{\mathcal{M}^2 - t}{s(p_T^2 + M^2)}\right]^{1-2\alpha_{AC}(t)}$$

where $x = -t/(s+u)$.

In the triple Regge limit defined by $s \approx |u| \gg \mathcal{M}^2 \gg |t|$, x goes to zero, $p_T^2 \sim -t$, and one finds the familiar Mueller-Regge form[16]

$$E\frac{d\sigma^q}{d^3p} = \beta_q(t)\,(xG_{q/B}(x))_{x=0} \left(\frac{\mathcal{M}^2 - t}{s}\right)^{1-2\alpha_{AC}(t)} .$$

In this limit, the inclusive cross section is independent of the threshold $(x \sim 1)$ behavior of the probability functions. However, we have already seen that it is this threshold behavior which allows a smooth connection to the exclusive $(\mathcal{M}^2 \sim 0)$ limit for both fixed t and fixed angle. The triple Regge formula does not allow for this smooth connection. It is guaranteed by multiplying by the simple function $xG_{q/B}(x)$. We have therefore identified an important correction to the triple Regge formula for small missing mass (which has the virtue of being particularly simple).

VIII. BRIEF REVIEW AND ASIDE

It is important to keep in mind the division we have made between internal or short distance properties (which predicts the irreducible processes discussed before) and the long distance or hadronic sector of strong interactions. Any theory that gives results for the irreducible processes that can be written in the following forms

1. Exclusive $$\frac{d\sigma}{dt} \propto (F^q_{BD}(t))^2 \frac{d\sigma}{dt}(A + q \to C + q)\Big|_{\substack{s' = \langle x\rangle s \\ u' = \langle x\rangle u \\ t' = t}}$$

2. Inclusive $$E\frac{d\sigma}{d^3p} \propto \frac{s}{s+u}\sum_q xG_{q/B}(x)\frac{d\sigma}{dt}(A + q \to C + q)\Big|_{\substack{s' = xs \\ u' = xa \\ t' = t}}$$

3. Probability function $G_{H/A}(z) \propto z^{-\alpha(0)}(1-z)^{q(H/A)}$,

(where the quantity $d\sigma/dt\ (A + q \to C + q)$ is power behaved) will produce all the predictions for elastic single particle inclusive to be discussed shortly. If one is willing to assume the above forms, or to assume a model that relates them to simple quantities such as form factors, then the concept of constituent need never be used. However, the constituent interchange model has the virtue of predicting very simple relations between the limiting forms of all the functions involved which are quite specific since they depend only on the number of constituents involved.

One of the most puzzling aspects of the CIM (aside from the fact that no constituents have been seen) is the fact that even though there is strong binding involved, the constituents of one hadron do not seem to interact strongly with those in another hadron. This was first suggested in our original paper on the subject to explain the large ratio of pp to $\bar{p}p$ and K^+p to K^-p scattering at large angles, and then used to predict a leading p_T^{-8} behavior in $pp \to \pi X$ rather than the naturally expected scaling behavior of p_T^{-4}.[17] There is no fundamental understanding of how this happens. One possibility is that the basic theory has quarks and enjoys asymptotic freedom or is only asymptotically scale-free but it is not yet clear how this would work in detail. Another possibility is a class of quark containment theories (that might be termed container theories) in which the quarks interact strongly with the box that they are in but not with each other. Constituent interchange is then the natural force in such theories. There seems to be many analogies between such theories and independent particle models of the nucleus.

It is hoped that by examining models and their calculational rules, one can get clues as to the required behavior of a fundamental and complete theory of hadrons and their interactions. From this point of view, the "odder" the calculational rule, perhaps the better the clue.

IX. CENTRAL REGION

In order to get particles into the central region, it is advantageous to let both incident particles A and B bremsstrahlung, lose momentum and collide at a low relative effective energy. This type of inclusive process is conveniently decomposed into peripheral interactions, hadronic bremsstrahlung and the basic irreducible process as illustrated in Fig. 14. A very large class of theories can be decomposed in this fashion; for example, many of the statistical models can be so written. The resulting cross section is obviously of the form

$$E\frac{d\sigma}{d^3p}(A + B \to C + x)$$
$$= \sum_{a,b}\int dx\,dy\, G_{a/A}(x)\, G_{b/B}(y)\, E\frac{d\sigma^I}{d^3p}(a + b \to C + d^*)\Big|_{\substack{s' = xys \\ t' = xt \\ u' = yu}}$$

and

$$M_a^2 + M_b^2 + M_C^2 + M_{d^*}^2 = xys + xt + yu\ .$$

The irreducible process $a + b \to C + d^*$ (no extra hadrons are allowed to be emitted) can be conveniently separated into contributing graphs as depicted in Fig. 15. The first term on the right is the pure fixed power behaved amplitudes previously discussed while the second term gives rise to Regge behavior

for the process $a + q \to C + q$. The third term corresponds to the production of a state c in the basic interaction that subsequently decays to the observed particle C.

Using the relation between the irreducible and total probability functions,

$$G_{q/B}(x) = \int_x^1 \frac{dz}{z} \sum_b G^I_{q/b}(\tfrac{x}{z})\, G_{b/q}(z) \ ,$$

the inclusive cross section can be written in the convenient but unsymmetrical form

$$E\frac{d\sigma}{d^3p}(A + B \to C + x) = \int_{z_c}^1 dz \sum_a G_{a/A}(z)\, E\frac{d\sigma}{d^3p}(a + B \to C + x) \ ,$$

where $z_0 = -u/(s+t)$ and the inclusive cross section under the integral is evaluated at $s' = zs$, $u' = u$, and $t' = zt$. In this formula, small intermediate transverse momenta have been neglected, and the required symmetrization between the particles has not been explicitly denoted. This is easily handled in any specific reaction of interest.

The general behavior of the inclusive cross section can be understood from quite simple kinematic arguments that are of course implicitly contained in the above formula. The basic (internal) process is $a + q \to C + q$ and it has an $(\text{energy})^2$ of

$$s_{eff} = xys \sim \frac{x^2(-u)s}{xs + t} \geq 4p_T^2 \ ,$$

if the missing mass M_{d^*} is kept finite. Therefore this process is operating at a fixed angle and at an $s_{eff} \sim 4p_T^2$, and one expects

$$\frac{d\sigma}{dt}(a + q \to C + q) \sim (p_T^2)^{-N} f(\theta)$$

where N is related to the total number of constituents involved in this subreaction. Thus the p_T dependence of the inclusive cross section is related to and determined by the number of constituents involved in the basic process. Let us now discuss the behavior of the cross section given by the above integral more carefully in various kinematic regions.

Let us first examine the central region where $p_T^2 \sim tu/s \sim$ constant, and $\epsilon = \mathcal{M}^2/s \sim 1$. The integral over z is easily estimated in the above formula and one finds

$$E\frac{d\sigma}{d^3p} = \sum_a g_a(x_L, \epsilon)(p_T^2)^{-N_a}$$

where $N_a \equiv 2(1 - \alpha_{AC}(\langle z\rangle t))$, and $\langle z\rangle$ is the average value of z involved in the integral. For large $|t|$, $\alpha_{HC} \approx \alpha_{HC}(-\infty)$ which is a number determined by counting. For example, $\alpha_{AC} = -1$ yields p_T^{-8} terms, $\alpha_{AC} = -2$ yields p_T^{-12} terms, etc.

A second interesting region is the threshold region defined by $\epsilon \to 0$. This limit should suppress the bremsstrahlung contributions and one finds that this is indeed the case. Note that the suppression works from both ends of the integral since $z_0 = 1 - \epsilon/(1 + t/s) \to 1$, and also, the x variable in the inclusive process under the integral is

$$x' = -\frac{t'}{s' + u'} = \frac{(z - z_0)(s+t)}{(zs + u)} \ .$$

Thus in the integrand, $z \sim z_0$ is suppressed and of course $z \sim 1$ is suppressed by the explicit $G(z)$ probability function. One finds

$$E\frac{d\sigma}{d^3p} \simeq \sum_{a,b} \epsilon^{F(a,b)}\, r_{ab}(p_T, u/s)$$

where

$$F(a,b) = g(\tfrac{a}{A}) + g(\tfrac{b}{B}) + 1 \ .$$

A more careful analysis of the integral yields the behavior for the a, b contribution

$$\sim \epsilon^{F(a,b)}(p_T^2 + M^2)^{-N_a} \left(\frac{1}{4} x_T^2 + \bar{y}\epsilon\right)^{1-g(b/B)-2\bar{\alpha}} f(p_T, \theta)$$

where $0 < \bar{y} < 1$ (using the mean value theorem)and $\bar{\alpha} \equiv \alpha(\langle z\rangle t)$. Note that if $x_T^2 \gg \epsilon$, which is true in the deep scattering regions, then the ϵ dependence is given by the first factor; however, if $x_T^2 \ll \epsilon$, which is true as one approaches the triple Regge region, then one finds a different power of ϵ. This can be interpreted as a triple Regge formula with an effective trajectory given by

$$\alpha_{eff}(t) = \alpha_{AC}(\langle z\rangle t) - \frac{1}{2}[1 + g(a/A)]$$

which can be described as a nonleading Regge (disconnected cut) contribution.

We have now identified a second important correction to the triple Regge formula which should become important at large missing mass and provides the correct extrapolation into the central region. An analysis of reactions of the form $pp \to CX$, where $C = p, \pi^{\pm}, K^{\pm}, \bar{p}$, has been carried out by Chen, Wang, and Wong.[19] As discussed in more detail in Ref. 4, their results for the effective trajectory provide evidence for the type of correction we are discussing and for the quantum number dependence predicted by the above formula for α_{eff}.

X. CHARACTERIZATION OF CROSS SECTIONS

It is convenient to have a simple way to characterize the possible behaviors of the inclusive cross section arising from different basic processes. If one includes the case in which the final particle C is a decay product of particle c, then one finds at large p_T that

$$E\frac{d\sigma}{d^3p} = \sum_{a,b,c} \frac{\epsilon^F}{(p_T^2 + M^2)^N} I_{a,b}\left(\epsilon, \frac{u}{s}\right)$$

where

$$F = 2(n(\bar{a}A) + n(\bar{b}B) + n(\bar{c}C)) - 1$$

$$N = n_a + n_b + n_c + n_{d^*} - 2$$

and $I_{a,b}$ is a slowly varying function. It will be set equal to a constant from now on in our discussion but is needed in any detailed numerical fit,[20] especially for values of x_L not near zero.

Some sample values of F and N are given in Tables I and II. The two numbers F and N have a simple physical interpretation. The power N measures the number of fundamental fields in the basic interaction that must act coherently in order to produce the observed large p_T. The power F measures the forbiddeness, or the number of fields that must be radiated by the incident systems A and B to arrive at the given subprocess plus the number that must be radiated in the final state produce the observed particle C.

In order to clarify these tables, consider some basic processes and the types of reactions that they can contribute to (M = any nonexotic meson state):

N = 4 (6 quarks involved):

$M + q \to \pi + q$

$\bar{q} + q \to \pi + M$

$q + q \to B + \bar{q}$

N = 6 (8 quarks involved):

$M + M \to \pi + M^*$

$q + (qq) \to \pi + B^*$

$B + q \to B + q$

N = 8 (10 quarks involved)

$B + M \to B + M^*$

$B + (qq) \to B + (qq)$.

TABLE I

Inclusive Process	Exclusive Limit Channel	Subprocesses	$\frac{d\sigma}{d^3p/E}$ $(\theta \sim 90°)$
$M + B \to M + X$	$M + B \to M + B^*$	$\underline{M + q \to M + q}$	$(p_\perp^2)^{-4}\ \epsilon^3$
	$(n = 10)$	$\bar{q} + B \to M + qq$	$(p_\perp^2)^{-6}\ \epsilon^1$
		$M + B \to M + B$	$(p_\perp^2)^{-8}\ \epsilon^{-1}$
$B + B \to B + X$	$B + B \to B + B^*$	$\underline{B + q \to B + q}$	$(p_\perp^2)^{-6}\ \epsilon^3$
	$(n = 12)$	$B + (qq) \to B + qq$	$(p_\perp^2)^{-8}\ \epsilon^1$
		$B + B \to B + B$	$(p_\perp^2)^{-10}\ \epsilon^{-1}$
	$B + B \to B + B^* + M^*$	$\underline{q + q \to B + \bar{q}}$	$(p_\perp^2)^{-4}\ \epsilon^7$
	$(n = 14)$	$q + (qq) \to B + M$	$(p_\perp^2)^{-6}\ \epsilon^5$
		$(qq) + B \to B + M + qq$	$(p_\perp^2)^{-10}\ \epsilon^1$
		$B + B \to B + B + M$	$(p_\perp^2)^{-12}\ \epsilon^{-1}$

The expected dominant subprocesses for selected hadronic inclusive reactions at large transverse momentum. The second column lists the important exclusive processes which contribute to each inclusive cross section at $\epsilon \sim 0$. The basis subprocesses expected in the CIM, and the resulting form of the inclusive cross section $Ed\sigma/d^3p \sim (p_\perp^2)^{-N}\ \epsilon^P$ for $p_\perp^2 \to \infty$, $\epsilon \to 0$, and fixed θ_{cm} are given in the last columns. The subprocesses that have the dominant $p_\perp$ dependence at fixed ϵ are underlined.

TABLE I Cont.

Inclusive Process	Exclusive Limit Channel	Subprocesses	$\frac{d\sigma}{d^3p/E}$ $(\theta \sim 90°)$
$B + B \to M + X$	$B + B \to M + B^* + B^*$	$\underline{q + (qq) \to M + B^*}$	$(p_\perp^2)^{-6}\ \epsilon^6$
	$(n = 14)$	$q + B \to q(\to M + q) + B^*$	$(p_\perp^2)^{-6}\ \epsilon^5$
		$q + B \to M + q + B^*$	$(p_\perp^2)^{-8}\ \epsilon^3$
		$(qq) + B \to M + B^* + qq$	$(p_\perp^2)^{-10}\ \epsilon^1$
		$B + B \to M + B^* + B^*$	$(p_\perp^2)^{-12}\ \epsilon^{-1}$
	$B + B \to M + M^* + B^* + B^*$	$\underline{M + q \to M + Q}$	$(p_\perp^2)^{-4}\ \epsilon^9$
	$(n = 16)$	$q + q \to \bar{q}(\to M + \bar{q}) + B^*$	$(p_\perp^2)^{-4}\ \epsilon^9$
		$q + q \to M + B^* + \bar{q}$	$(p_\perp^2)^{-6}\ \epsilon^7$
		$M + B \to M + B^*$	$(p_\perp^2)^{-8}\ \epsilon^5$
	$B + B \to M + M^* + M^* + B^* + M^*$	$\underline{q + \bar{q} \to M + M^*}$	$(p_\perp^2)^{-4}\ \epsilon^{11}$
	$(n = 18)$	$q + M \to q(\to M + q) + M^*$	$(p_\perp^2)^{-4}\ \epsilon^{11}$
$B + B \to \bar{B} + X$	$B + B \to \bar{B} + B^* + B^* + B^*$	$\underline{q + q \to B^* + \bar{q}(\to \bar{B} + qq)}$	$(p_\perp^2)^{-4}\ \epsilon^{11}$
	$(n = 18)$	$q + q \to B^* + \bar{B} + qq$	$(p_\perp^2)^{-8}\ \epsilon^7$
		$q + (qq) \to \bar{B} + B^* + B^*$	$(p^2)^{-10}\ \epsilon^5$

TABLE II

Inclusive Process	Exclusive Limit Channel	Subprocesses	$\frac{d\sigma}{d^3p/E}$ $(\theta \sim 90°)$
$\gamma + B \to \gamma + X$	$\gamma + B \to \gamma + B^*$	$\underline{\gamma + q \to \gamma + q}$	$(p_\perp^2)^{-2}\ \epsilon^3$
	$(n = 8)$	$\gamma + B \to \gamma + B^*$	$(p_\perp^2)^{-6}\ \epsilon^1$
		$\bar{q} + B \to \gamma + qq$	$(p_\perp^2)^{-5}\ \epsilon^0$
	$\gamma + B \to \gamma + B^* + M^*$	$q + (qq) \to B^* + \gamma$	$(p_\perp^2)^{-5}\ \epsilon^2$
	$(n = 10)$	$q + B \to B^* + \gamma + q$	$(p_\perp^2)^{-7}\ \epsilon^0$
		$\bar{q} + q \to M + \gamma$	$(p_\perp^2)^{-3}\ \epsilon^4$
		$\gamma + (qq) \to B^* + \gamma + \bar{q}$	$(p_\perp^2)^{-6}\ \epsilon^1$
$\gamma + B \to M + X$	$\gamma + B \to M + B^*$	$\underline{\gamma + q \to M + q}$	$(p_\perp^2)^{-3}\ \epsilon^3$
	$(n = 9)$	$\bar{q} + B \to M + qq$	$(p_\perp^2)^{-6}\ \epsilon^0$
		$\gamma + B \to M + B^*$	$(p_\perp^2)^{-7}\ \epsilon^{-1}$
	$\gamma + B \to M + M^* + B^*$	$\gamma + (qq) \to B^* + M + \bar{q}$	$(p_\perp^2)^{-7}\ \epsilon^1$
	$(n = 11)$	$\bar{q} + q \to M + M^*$	$(p_\perp^2)^{-4}\ \epsilon^4$
		$q + (qq) \to M + B^*$	$(p_\perp^2)^{-6}\ \epsilon^2$

The expected dominant subprocesses for selected electromagnetically induced reactions at large transverse momentum. (See Table I.)

TABLE II Cont.

Inclusive Processes	Exclusive Limit Channel	Subprocesses	$\frac{d\sigma}{d^3p/E}$ $(\theta \sim 90°)$
$\gamma + B \to B + X$	$\gamma + B \to B + M^*$	$\underline{\gamma + (qq) \to B + \bar{q}}$	$(p_\perp^2)^{-5}\ \epsilon^1$
	$(n = 9)$	$q + B \to B + q$	$(p_\perp^2)^{-6}\ \epsilon^0$
		$\gamma + B \to B + M^*$	$(p_\perp^2)^{-7}\ \epsilon^1$
	$\gamma + B \to B + M^* + M^*$	$\underline{q + q \to B + \bar{q}}$	$(p_\perp^2)^{-4}\ \epsilon^4$
	$(n = 11)$	$\gamma + q \to B + \bar{q}\bar{q}$	$(p_\perp^2)^{-5}\ \epsilon^3$
		$q + (qq) \to B + M^*$	$(p_\perp^2)^{-6}\ \epsilon^2$
$e + B \to e + X$	$e + B \to e + B^*$	$e + q \to e + q$	$(p_\perp^2)^{-2}\ \epsilon^3$
	$(n = 8)$		
	$e + B \to e + B^* + M^* + M^*$	$e + \bar{q} \to e + \bar{q}$	$(p^2)^{-2}\ \epsilon^7$
	$(n = 12)$		

The dominant terms in the reactions of the type $pp \to CX$, where $C = \pi^{\pm,0}, K^{+}, \rho^{\pm,0}$, etc. are expected to be of the form shown in Fig. 16, with $N = 4, 6$, and 4 respectively. It is a simple matter to count the minimum possible bremsstrahlung states and one finds

$$E\frac{d\sigma}{d^3p} = (p_T^2 + M^2)^{-4}\,[h_1\epsilon^9 + h_2\epsilon^{11}] + (p_T^2 + M^2)^{-6}\,h_3\epsilon^5 + \cdots$$

The constants h_1, h_2, and h_3 vary from process to process. For the reaction $pp \to K^-X$ on the other hand, the initial state has no quarks in common with those in K^- and more bremsstrahlung is necessary, hence

$$E\frac{d\sigma}{d^3p}(K^-) = (p_T^2 + M^2)^{-4}\,[h_1\epsilon^{13} + h_2\epsilon^{11}] + (p_T^2 + M^2)^{-6}\,h_3\epsilon^9 .$$

Note that if the h_2 term dominated both the K^- and K^+ reactions, their ratio (K^-/K^+) would be independent of $x_\perp$. In general, however, one expects that this ratio will fall as $\epsilon \to 0$ (or increasing $x_\perp$) by a factor of ϵ^2 or ϵ^4 (if one had to guess). This latter behavior agrees with the qualitative behavior of the Chicago-Princeton data.[21]

This characterization of the data emphasizes that there are two distinct limits involved here. They are:

(1) p_T large (ϵ fixed), where the minimum value of N dominates

(2) $\epsilon \to 0$ (p_T fixed), where the minimum value of F dominates.

It is often stated that <u>the</u> parton model (whatever that is) predicts a factorization of the form ($x_L = 0$, p_T large and N = constant)

$$E\frac{d\sigma}{d^3p} \simeq (p_T^2 + M^2)^{-N}\,f(\epsilon) .$$

We see that this statement has a grain of truth but is not correct. It is oversimplified both physically and mathematically. However, a single term may happen to dominate in a certain regime. In any case, it is convenient to analyze data by assuming the above form and determining the effective value of N as a function of s, p_T, or ϵ. Defining N_{eff} by varying p_T^2 (or s) at fixed ϵ,

$$N_{eff} \equiv -\,p_T^2\frac{\partial}{\partial p_T^2}\ln\left(E\frac{d\sigma}{d^3p}\right) ,$$

one finds by using a single term form that

$$N_{eff} = N\left(1 + \frac{M^2}{p_T^2}\right)^{-1} .$$

This simple curve has the qualitative features of the N_{eff} extracted by the Chicago-Princeton group (see also the talk by Cronin in these proceedings) if M^2 is a few $(\mathrm{GeV})^2$. One also sees that more than one term is probably needed to accurately fit the data.

Let me now show you some rough fits to the data that I have carried out. These are not optimum fits in any sense, the parameters were simply varied until the theoretical curves looked something like the data for $pp \to \pi^-X$. The procedure used was as follows. I arbitrarily set $h_2 = 0$ even though by retaining it, a better fit could be achieved at intermediate values of p_T. The constants h_1 and h_3 were fit to the Chicago-Princeton-FNAL data[21] at large p_T (~ 5-6 GeV/c) and then the mass parameters associated with the p_T^2 denominators were chosen to agree with the data for $p_T \sim 1$ GeV/c. The resultant curves for the 200, 300, and 400 GeV/c data is shown in Fig. 17 along with the experimental points. Roughly speaking, the p_T^{-8} and the p_T^{-12} terms are comparable throughout this regime but the p_T^{12} term always wins at large p_T due to its slower falloff in ϵ. If one uses only the p_T^{-8} term, the fit is as shown in Fig. 18. One should take note of the fact that there are important nuclear effects in the data which effect the lower p_T range and primarily the magnitude of h_3. Take all details of these "fits" with a grain of salt.

In the upper ISR range of energies, the p_T^{-12} term is negligible ($\epsilon > 0.6$ for this data), and the agreement with the data[22] is excellent for $\sqrt{s} \gtrsim 30.6$ GeV as is shown in Fig. 19. An important question is whether low energy accelerator data is exploring the same physics as the ultra high energy data discussed above. The answer seems to be in the affirmative but low energy data does not exist for the most part, and much more is needed. In Figs. 20 and 21, the predictions of the theory using the same parameters as determined above are shown as dotted lines and compared with the data of Allaby, et al.[23] at 24 GeV/c. These curves check two aspects of the theory, the overall normalization (and its (scaling) energy dependence) and the behavior away from $x_L = 0$. The agreement is much better than could be expected. For increasing $x_L \gtrsim 0.5$, triple Regge and leading particle effects come in as expected and the agreement rapidly worsens. In fitting this data, the function $I(x,y)$ is quite important in determining the $x_L \neq 0$ behavior. Finally, the predictions at 69 GeV/c are in quite good agreement with the recent results of the Saclay-Serpuhkov collaboration[24] for $p_T < 1.25$ GeV/c and $x_L = 0$ as is shown in Fig. 22. When the effects of nuclear absorption on the Chicago-Princeton data are accurately understood, it will be necessary to go back and perform a careful fit of all of this data. It should be stressed that the low energy data is a powerful constraint on the theory and should not be ignored (as most theorists in this game seem to do).

B.

The reaction $pp \to pX$ is an interesting one because it involves a more coherent final state particle and has quite a few subprocesses that can contribute significantly to it (see Table I). The basic process $q + q \to B + \bar{q}$ will ultimately produce a p_T^{-8} behavior if it is present at all. However, since the original process may be in some sense close to its exclusive limit, one would expect that the diagrams that were shown to dominate the exclusive process should be important in the inclusive case, particularly for small ϵ. The dominant exclusive diagrams are shown in Fig. 23 and their immediate inclusive analogues in Fig. 23b. Notice that the two final states are different and incoherent for fixed ϵ since one involves a recoil q while the other involves a recoil "core." These will contribute terms of the order of p_T^{-12} and p_T^{-16} respectively. Retaining these three basic contributions only (which may be too drastic), the cross section in the central region should be characterized by the form

$$E \frac{d\sigma}{d^3p}(p)$$

$$= (p_T^2 + M^2)^{-4} h_1 \epsilon^7 + (p_T^2 + M^2)^{-6} [h_2 \epsilon^3 + h_4 \epsilon^5] + (p_T^2 + M^2)^{-8} [h_3 \epsilon^1 + h_6 \epsilon^3] + \cdots,$$

where h_4 and h_6 are additional (Feynman) scaling contributions arising from bremsstrahlung of the initial beam protons. The N_{eff} analysis of the data by Cronin at this conference indicates that the h_3, h_6 terms seems to dominate the amplitude for $\epsilon < 1/2$. This process has not been carefully analyzed, and one should be able to learn a lot from it. Perhaps large p_T data from the ISR will tell us whether the very interesting h_1 term is present, for example. Note also that in the exclusive limit, the h_2 and h_3 terms contribute to order s^{-10} while the h_1, h_4, and h_6 terms are nonleading at s^{-12}. A detailed discussion of the particle ratios will shortly be published.[25]

C.

One of the most interesting features of the CIM is the strong dependence of the predicted powers on the quantum numbers of the particles involved. In the previous sections, we have seen how the powers vary as a function of the detected particle. Similar effects should occur if various beam particles are utilized, and this should provide a severe test of the entire approach. For example, the reaction $\pi p \to \pi X$, the presence of antiparticles in the initial

state means that less bremsstrahlung is required and the process is less forbidden than $pp \to \pi X$ but it involves the same basic processes. The cross section is expected to be of the form

$$E \frac{d\sigma}{d^3p} (\pi p \to \pi x)$$

$$= (p_T^2 + M^2)^{-4} [h_1\epsilon^7 + h_2\epsilon^5 + h_3\epsilon^3] + (p_T^2 + M^2)^{-6} [h_4\epsilon^3 + h_5\epsilon] + \cdots .$$

The h_3 and h_5 terms do not Feynman scale and contribute to the exclusive limit s^{-8} behavior. They involve the subprocesses $(\pi + q \to \pi + q)$ and $(\bar{q} + p \to \pi + \text{core})$ respectively, and an extra factor of $x_T^2 = (1-\epsilon)^2$ should be included for all such nonscaling terms but has been dropped for simplicity.

Another interesting case is the reaction $\bar{p}p \to \pi X$, which involves some new possibilities for the subprocesses. The cross section takes the form

$$E \frac{d\sigma}{d^3p} (\bar{p}p \to \pi X)$$

$$= (p_T^2 + M^2)^{-4} [h_1\epsilon^9 + h_2\epsilon^7] + (p_T^2 + M^2)^{-6} [h_3\epsilon^3 + h_4\epsilon^5 + h_5\epsilon^1] + \cdots .$$

The term h_3 arises from the interesting and unusual process $\text{core} + \overline{\text{core}} \to \pi + \pi$, and h_4 from $\bar{q} + \text{core} \to \pi + q$. The h_5 term (which does not Feynman scale) is the only one that contributes to an s^{-8} behavior in the exclusive limit and involves the processes $(\bar{p} + \text{core} \to \pi + \bar{q})$ and $(p + \overline{\text{core}} \to \pi + q)$.

D.

Processes involving photons are particularly important since they should most clearly probe the point-like nature of the constituents. The parton concept was invented in the first place to explain Bjorken scaling of the deep inelastic structure functions! A glance at Table II should convince you that there are a large number of experimental and theoretical possibilities here also. Let me confine my remarks to a brief discussion of two inclusive processes, photo-pion production and compton scattering although exclusive processes are extremely interesting. In Fig. 24 the conventional and expected contributions to these processes arising from (a) $\gamma + q \to \pi + q$ and (b) $\gamma + q \to \gamma + q$ are illustrated with the additional, nonleading terms arising from the subprocesses $\bar{q} + B \to \pi + \text{core}$ and $\bar{q} + B \to \gamma + \text{core}$. Just as in the hadronic case, these types of diagrams are expected to be important, especially at small ϵ. They are perhaps easiest thought of as arising from the baryon scattering off of the $(\bar{q}q)$ components of a target photon. Actually all of these contributions arise from the same basic type of diagrams, but evaluated in different regions of phase space with different particles being far off mass shell, etc.

The expected cross sections are

$$E \frac{d\sigma}{d^3p} (\gamma p \to \pi X) = (p_T^2 + M^2)^{-3} J_1\epsilon^3 + (p_T^2 + M^2)^{-6} J_2\epsilon^0 + \cdots$$

and

$$E \frac{d\sigma}{d^3p} (\gamma p \to \gamma X) = (p_T^2 + M^2)^{-2} J_1'\epsilon^3 + (p_T^2 + M^2)^{-5} J_2'\epsilon^0 + \cdots$$

The ϵ^0 terms would be ϵ^1 if the photon were pure vector meson dominated (so that it would act like a $\bar{q}q$ state rather than a fundamental field).

The photoproduction process has been analyzed by Eisner et al.[27] at 21 GeV/c for π^0 and they find $N_{eff} \sim 6\text{-}7$ and $F_{eff} \sim 0.5$ with $M^2 \sim 0.5\text{-}1.2$. Boyarski et al.[28] have analyzed $\pi^\pm$, $K^\pm$, and $p^\pm$ data at 18 GeV/c and for the charged pion case find a reasonable fit with $N_{eff} \sim 6$ and $F_{eff} \sim 1$. The best fit varies slightly with the particular process under consideration.

The compton process is very interesting and a basic one for any parton model. The J_1' term is the Bjorken-Paschos process[29] which they showed can be used to measure the ratio $\langle Q_i^4 \rangle / \langle Q_i^2 \rangle$ where $\langle Q_i \rangle$ is average quark charge in the proton. However, one expects that sizable and even dominant (at present

energies) corrections will arise from terms of the form of the J_2' contribution. The J_1' term could still be extracted by a careful fitting of good data and this would be a very worthwhile project.

E.

In this section I would like to briefly review the general structure expected in inclusive final states that is expected on the basis of our previous discussion. A more extensive discussion will be given by Stan Brodsky in these proceedings and a numerical discussion will be published soon by J. Gunion. I will restrict myself to some qualitative remarks.[30] The general decomposition of the inclusive process is illustrated in Fig. 14 and Fig. 15. The basic interaction where the large p_T is generated involves the collision of two components of the incident hadrons. For example, the dominant term in the ISR range was shown to arise from the collision of a quark and a meson. In the overall center of mass, since the quark distribution function vanishes as $(1 - z)^3$ while the meson's vanishes as $(1-z)^5$, the quark will tend to have a higher average momentum than the meson. Therefore one does not expect back-to-back angular distributions in this frame--the quark will retain its excess longitudinal momentum if the pion is detected at 90°. The details of the distribution will depend on the angular behavior of the basic $q + \pi$ processes. When the recoiling quark connects to hadrons, they will smear out this already smeared out distribution. The events tend to be planer except that at each stage of extracting one particle from another (which must occur at least three times in a correlation experiment) there is a small transverse momentum introduced at each stage (this small transverse momentum was neglected in our discussion of the single particle inclusive case). We therefore see from the above arguments how particles correlated with a large p_T particle on the opposite side are expected to have a wide x_L (or rapidity) distribution and to be nonplaner. Only detailed fits to the data can find out if the physical picture works.

Notice that since one expects (Matthew's Theorem) that resonances (or perhaps even "clusters") are produced with roughly the same cross section as pions, there will be correlations on the same side with the large p_T particle as well. This is a very interesting point to check since it is a rather severe test of the theory. More detailed tests have been proposed by Sivers and Newmeyer for this region.[31]

We have found that the Chicago-Princeton data seems to be dominated by the subprocess with a meson-B^* final state. Therefore one expects to find large p_T pions correlated with baryons on the <u>opposite</u> and the <u>same</u> side (arising from the B^* decay).

XI. CONCLUSIONS

What has been achieved by the picture of strong interactions that we have been describing? Perhaps the most impressive point is a simple analytical description of inclusive and exclusive reactions valid at fixed angle and fixed momentum transfer. There are few parameters since dimensional counting (applied to one's favorite nucleon model) determines all limiting behaviors in a simple way. This, together with the fact that the CIM joins smoothly onto normal Regge theory at fixed t, puts many constraints on the forms the model can predict. The new dynamics has been isolated in the irreducible processes, and it was shown that if one gives the form of

(A) the exclusive basic process at fixed angle

(B) the probability functions $G_{H/A}(z)$,

the inclusive can be built up from the above and then the full amplitude constructed by using only the long range hadron states.

What are some of the important questions raised?

1. No fundamental deviation of the calculational rules, and reasons for:
   (a) weak q-q force, especially between hadrons,[32]
   (b) dimensional counting rules, especially in light of (a).

(c) What is the rule for "allowed" basic processes? For example, is $q + q \to B + \bar{q}$ and/or $q + (qq) \to q + (qq)$ allowed?

(d) How should hadron cores or the (qq) system be handled?

2. Can one calculate absolute normalizations of various subprocesses and then related different reactions absolutely? One needs to understand absorption processes and their effects for these calculations.

3. Who, what, where, and why are the constituents, if any?

References

1. J.F. Gunion, S.J. Brodsky, and R. Blankenbecler, Phys. Rev. D6, 2652 (1972); Phys. Letters 42B, 461 (1972); to help settle questions of covariance in the approach used above, see M. Schmidt, Phys. Rev. D9, 40 (1974).
2. J.F. Gunion, S.J. Brodsky, and R. Blankenbecler, Phys. Letters 39B, 649 (1972); Phys. Rev. D8, 287 (1973).
3. S.J. Brodsky and G.R. Farrar, Phys. Rev. Letters 31, 1153 (1973); V. Matveev, R. Muradyan, and A. Tavkhelidze, Nuovo Cimento Lettere 7, 719 (1973). See also Z.F. Ezawa, DAMPT preprint 7415 (1974).
4. R. Blankenbecler and S.J. Brodsky, SLAC-PUB-1430, Phys. Rev. (to be published).
5. H.M. Fried and T.K. Gaisser, Phys. Rev. D7, 741 (1973); H.M. Fried, B. Kirby, and T.K. Gaisser, Phys. Rev. D8, 3210 (1973). A.P. Contogouris, J.P. Holden, and E.N. Argyres, Plattsburgh preprint, 1974.
6. R. Blankenbecler, S.J. Brodsky, J.F. Gunion, and R. Savit, SLAC-PUB-1294 and 1378, Phys. Rev. D 4117 (1973). For a phenomenological investigation of Regge behavior, see J. Tran Thanh Van, J.F. Gunion, D. Coon and R. Blankenbecler, SLAC-PUB-1483 (to be published).
7. R. Savit and R. Blankenbecler (in preparation).
8. The data are from C. Baglin et al., Phys. Letters 47b, 85 and 98 (1973). A. Eide, et al., Nucl. Phys. B60, 173 (1973).
9. A. Lundby, CERN preprint 73-3788, submitted to the Fifth International Conference on High Energy Collisons, Stony Brook, New York (1973).
10. J.F. Gunion, University of Pittsburgh preprint (to be published).
11. The idea that the decay of the $(N\bar{N})$ system should be related to the nucleon structure function was introduced and discussed by E. Pelaquier, contribution to IX Rencontre de Moriond (1974), and Montpellier preprint PM/74/7.

12. W.S. Brockett et al., Phys. Letters B51, 390 (1974). I wish to thank W.R. Frisken for discussions about this data and its analysis. G.W. Brandenburg et al., Phys. Letters 44B, 305 (1973).

13. S.D. Drell and T.M. Yan, Phys. Rev. Letters 24, 181 (1970); G.B. West, Phys. Rev. Letters 24, 1206 (1970).

14. E.D. Bloom and F.J. Gilman, Phys. Rev. Letters 25, 1140 (1970).

15. Slightly different versions of this connection are given in J.D. Bjorken and J. Kogut, Phys. Rev. D8, 1341 (1973); D.M. Scott, DAMTP Preprint 73/37. Our result for diffraction scattering is different from the above treatments at small t.

16. A. Mueller, Phys. Rev. D2, 2693 (1970).

17. S.M. Berman, J.D. Bjorken, and J.B. Kogut, Phys. Rev. D4, 3388 (1971). See also D. Horn and M. Moshe, Nucl. Phys. B48, 557 (1972); 139 (1973); J. Kogut, G. Frye, L. Susskind, Phys. Letters 49B, 469 (1972); R.M. Barnett and D. Silverman, UCI Preprint, December 1973. See also W.R. Theis, Phys. Letters 42B, 246 (1972).

18. I wish to thank D. Sivers for pointing this out.

19. Min-Shih Chen, Ling-Lie Wang and T.F. Wong, Phys. Rev. D5, 1667 (1972).

20. D.C. Carey et al., NAL-PUB-74/48 and 74/49--submitted to Phys. Rev. Letters. Their fit would not seem to work at larger transverse momenta.

21. J.W. Cronin et al., Phys. Rev. Letters 31, 1426 (1973).

22. F.W. Busser et al., Phys. Letters 46B, 471 (1973). M. Banner et al., Phys. Letters 44B, 537 (1973). B. Alper et al., Phys. Letters 44B, 521 (1973). See also the FNAL data of J.A. Appel et al., Phys. Rev. Letters 33, 719 (1974).

23. J.V. Allaby et al., CERN Report No. CERN-TH-70-11 (1970), unpublished. E.W. Anderson et al., Phys. Rev. Letters 19, 198 (1967).

24. Collaboration France-Soviet Union, Phys. Letters 50B, 283 (1973).

25. J.F. Gunion, S.J. Brodsky, and R. Blankenbecler (in preparation).

26. R. Anderson et al., Phys. Rev. Letters 30, 627 (1973).

27. A.M. Eisner et al., UCSR preprints, July 1974.

28. A. Boyarski et al., contribution to the Cornell conference, 1972, and D. Sherden (private communication). A SLAC-PUB is in preparation.

29. J.D. Bjorken and E. Paschos, Phys. Rev. 185, 1975 (1969).

30. See also the brief discussion by S. Ellis, contribution to the XVII International Conference on High Energy Physics (London), July 1974 and CERN preprint Th.1908.

31. J.L. Newmeyer and Dennis Sivers, SLAC-PUB-1425, May 1974, submitted to Phys. Rev.

32. Interesting speculations in this regard have been recently discussed by Z.F. Ezawa and J.C. Polkinghorne, Cambridge preprint DAMTP74/20 and A. Weldon (unpublished).

Figure Captions

Fig. 1. Elastic scattering cross section at 5 GeV/c. Note size of pp relative to meson-proton scattering and the qualitatively different angular distribution of $\bar{p}p$ and K^-p scattering.

Fig. 2. Inelastic scattering cross sections at 5 GeV/c. Note that they become roughly equal at large $|t|$ but differ by orders of magnitude in the forward direction.

Fig. 3. Annihilation process at 5 GeV/c. The cross section for $\bar{p}p \to K^-K^+$ is roughly equal to the above in the forward hemisphere but has a small backward peak as expected.

Fig. 4. Test of factorizability of s and angle dependence and of the predicted angular distribution in the CIM.

Fig. 5. The Peyrou plot illustrating the main kinematic regions of interest.

Fig. 6. Wave function and form factor diagrams.

Fig. 7. Even-tempered operator for the form factor for (a) a two-particle state and (b) a three-particle state.

Fig. 8. Typical scattering diagrams for the even tempered scattering operator. Meson-meson scattering is illustrated in (a) and (b), with the latter showing a direct quark-quark interaction. Meson-baryon is illustrated in (c).

Fig. 9. Effective trajectory for pp scattering for s between 20 and 40 $(\mathrm{GeV})^2$ assuming $M \sim (-u)^{\alpha(t)}\,\beta(t)$.

Fig. 10. Effective trajectory for π^-p scattering for s between 10 and 20 $(\mathrm{GeV})^2$ assuming a linear combination of $(-u)^{\alpha}$ and $(-s)^{\alpha}$ terms.

Fig. 11. Diagrams given rise to characteristic angular distributions. The (ut) terms arise as in (a), the (st) terms as in (b), and the (t) (or s(t)) terms as in (c).

Fig. 12. Illustrating the close relation between (a) exclusive and (b) inclusive scattering.

Fig. 13. The irreducible interaction (a) and its iteration in the t-channel (b) which gives rise to Regge behavior.

Fig. 14. The general separation of an inclusive process into beam fragmentation $X(A\bar{a})$, target fragmentation $X(B\bar{b})$ and the irreducible process.

Fig. 15. Simplest diagrams contributing to the irreducible process.

Fig. 16. Main diagrams expected to contribute to the reaction $pp \to \pi X$. Note the different final states arising from these contributions.

Fig. 17. Rough fit to the Chicago-Princeton-FNAL data using p_T^{-8} and p_T^{-12} terms.

Fig. 18. Same as Fig. 17 but using only a p_T^{-8} term.

Fig. 19. The fit used in Fig. 17 and compared with the ISR results of the CCR collaboration.

Fig. 20. Some parameters as in Fig. 17 compared with the data of Allaby, et al. The solid curves are data at constant p_T and the dashed lines are the theory for negative pions.

Fig. 21. Same as above but for the positive pion final states.

Fig. 22. Same parameters as in Fig. 17 compared with the negative pion data of the France-Soviet Union collaboration.

Fig. 23. Expected dominant diagram for (a) pp elastic scattering and (b) their corresponding form for inelastic scattering.

Fig. 24. Expected dominant diagrams for inclusive (a) photo-meson production and (b) compton scattering. The last diagram in each row is a type of important but nonleading process that seems to dominate the present data.

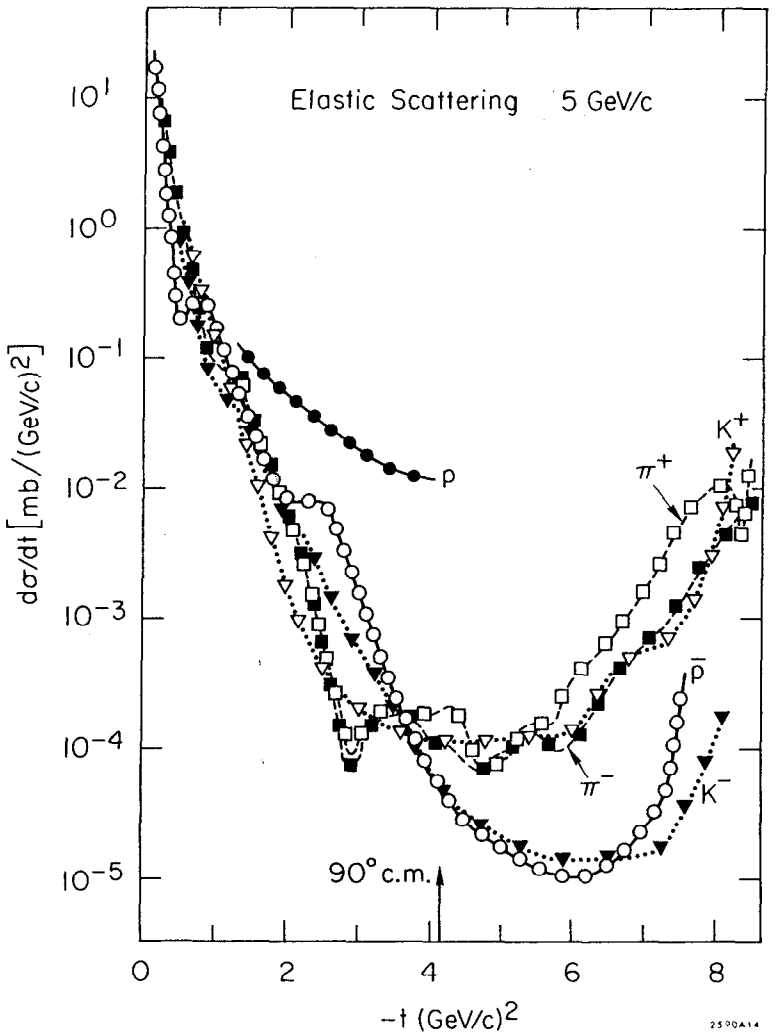

Figure 1

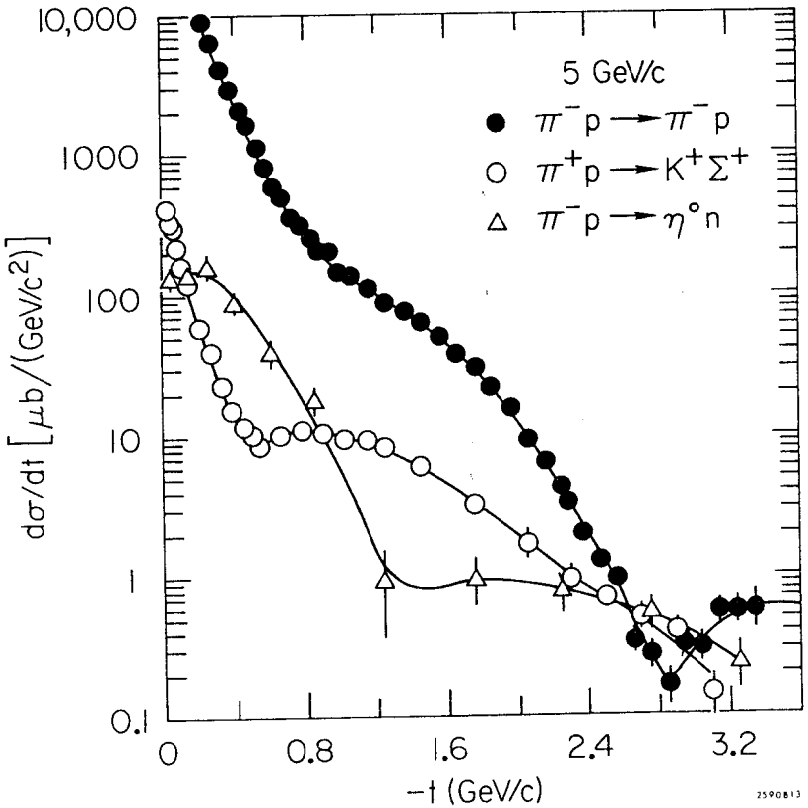

Figure 2

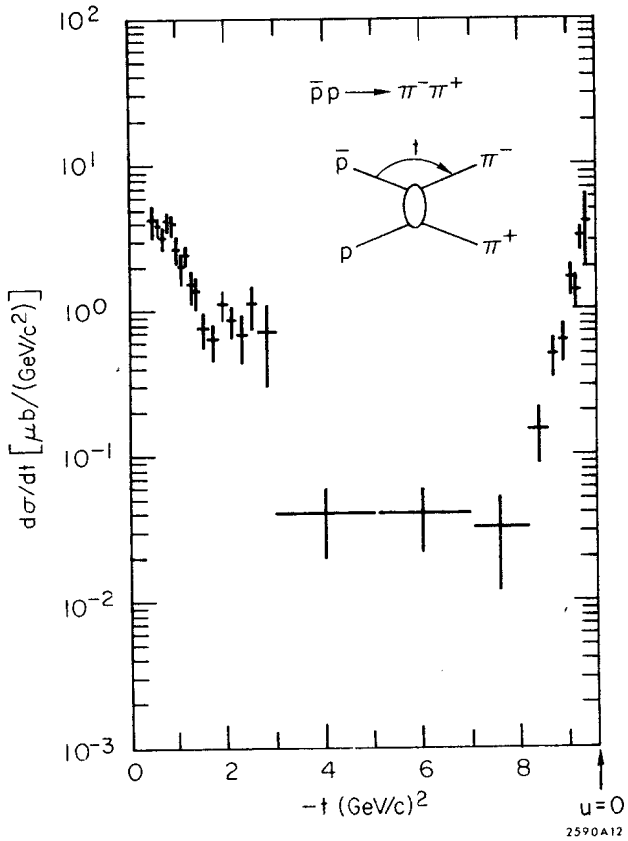

Figure 3

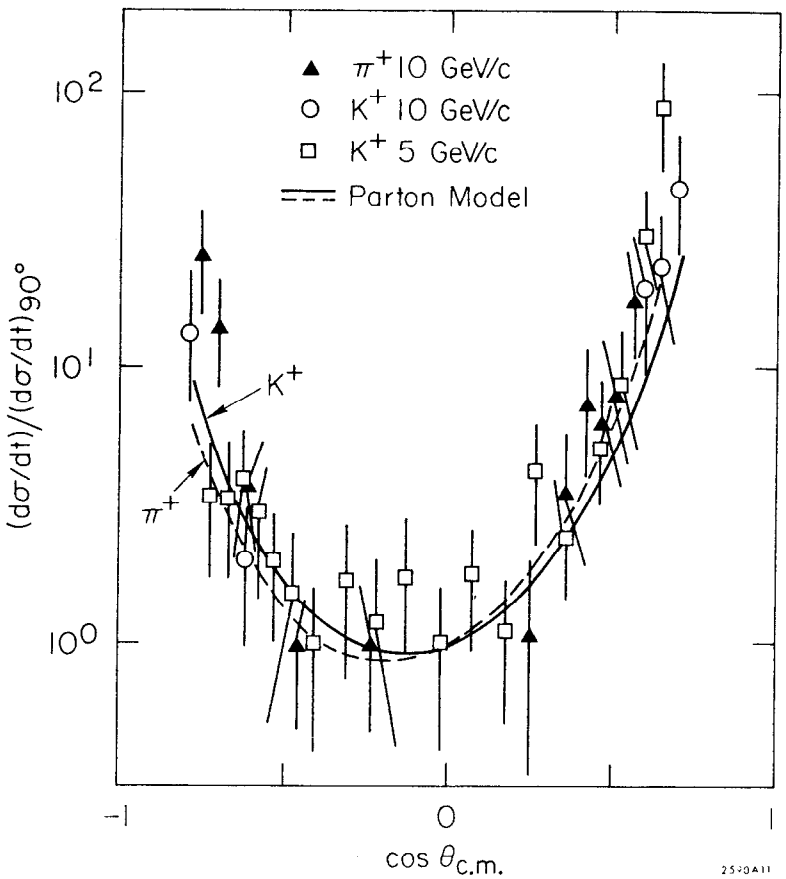

Figure 4

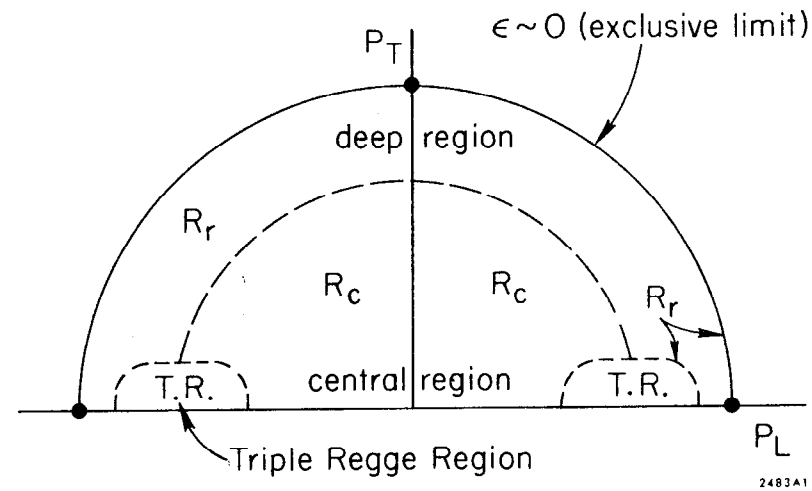

Figure 5

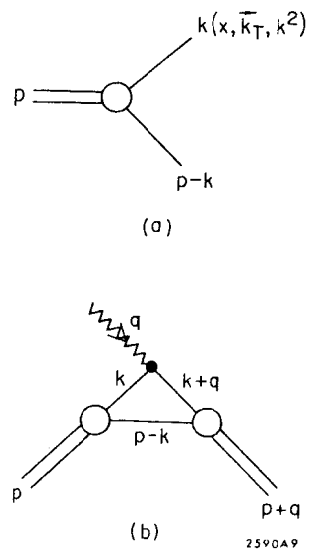

Figure 6

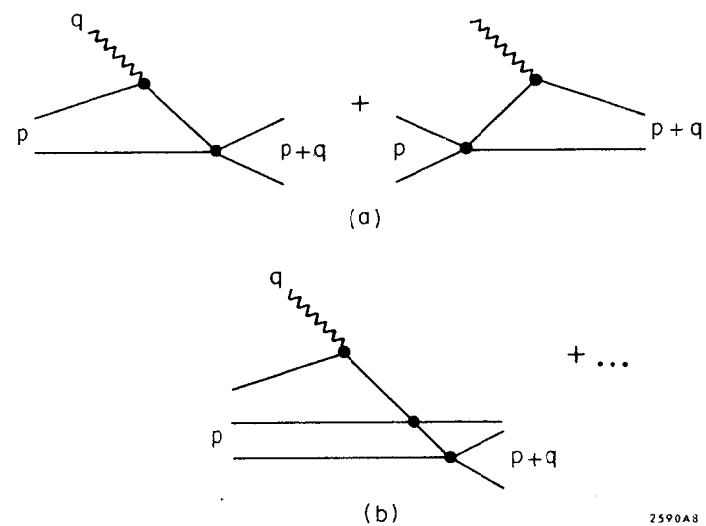

Figure 7

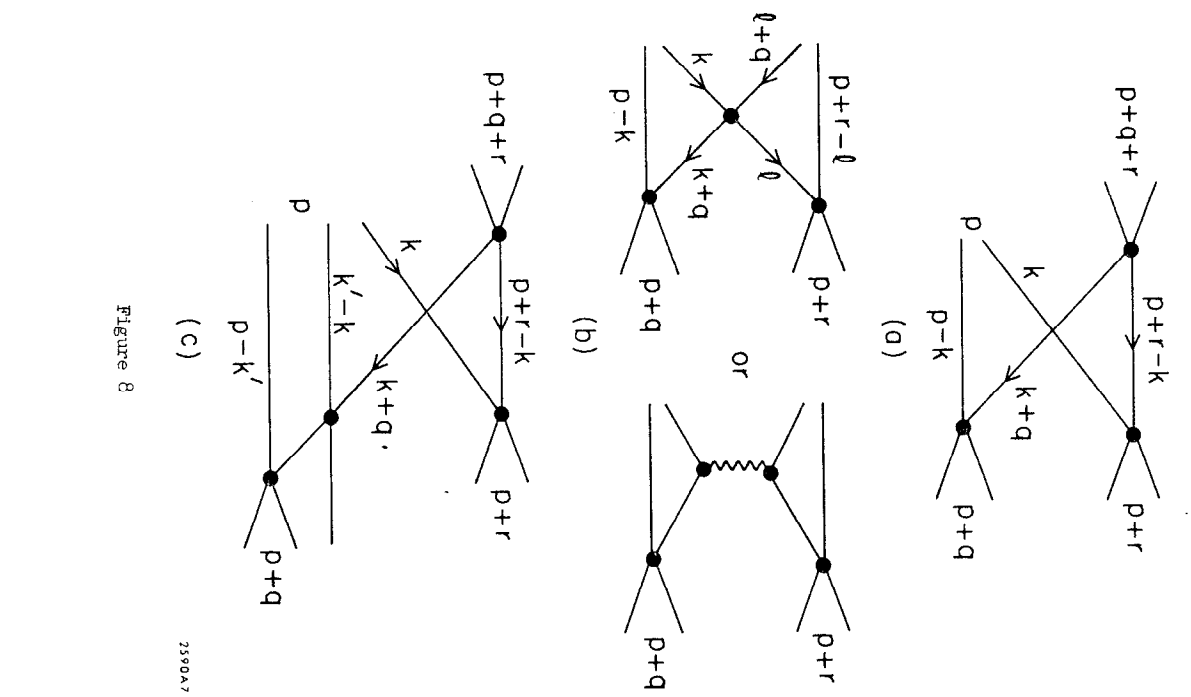

Figure 8

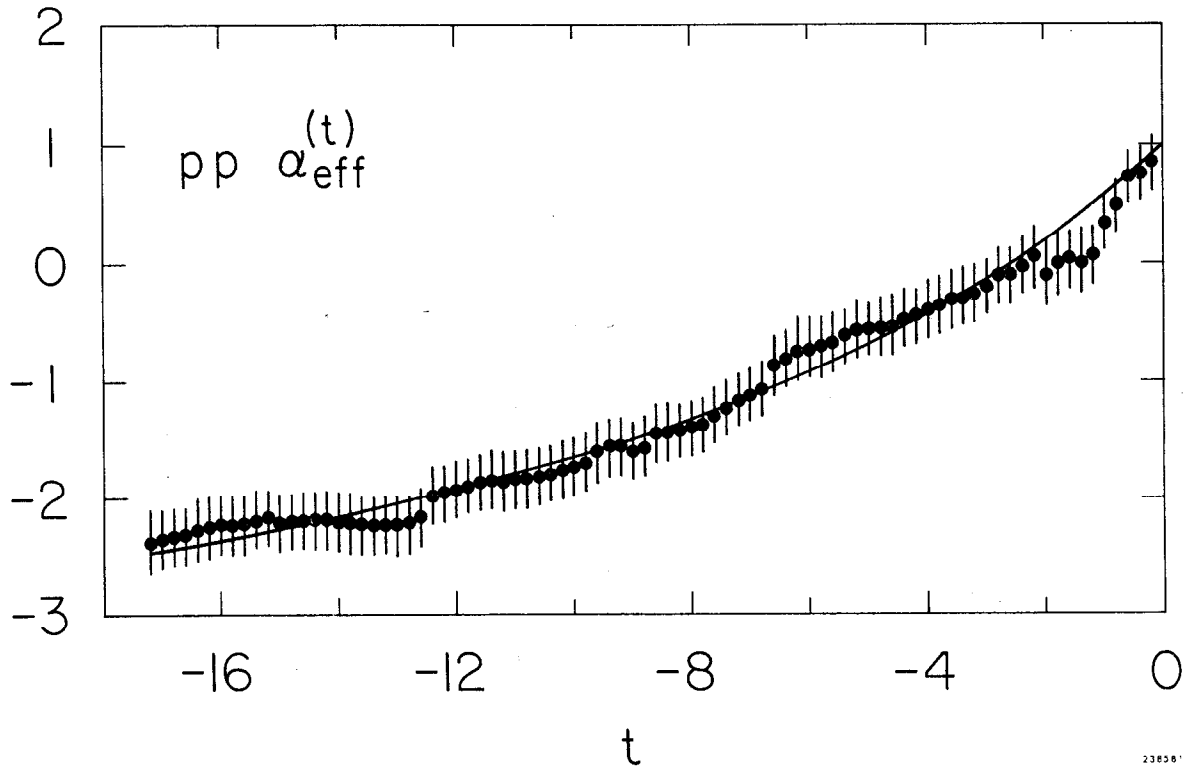

Figure 9

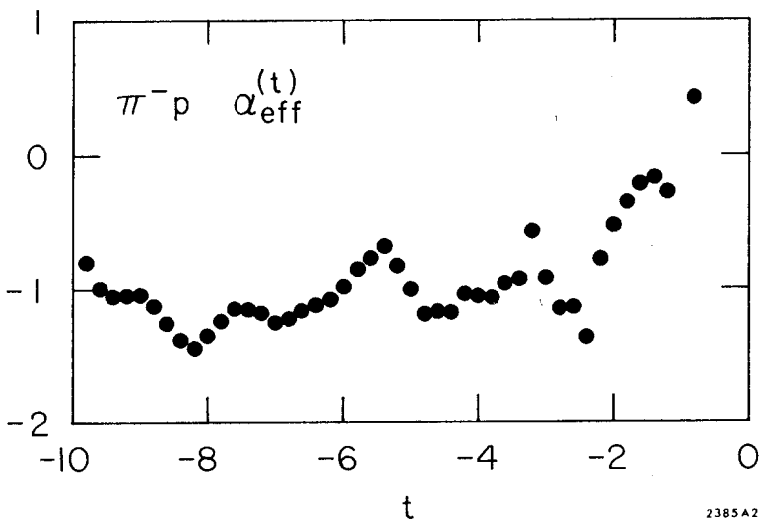

Figure 10

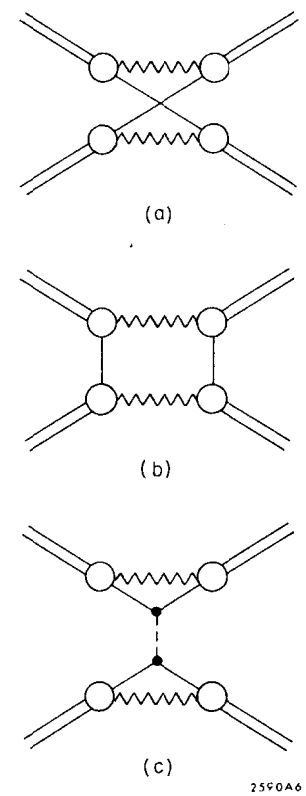

Figure 11

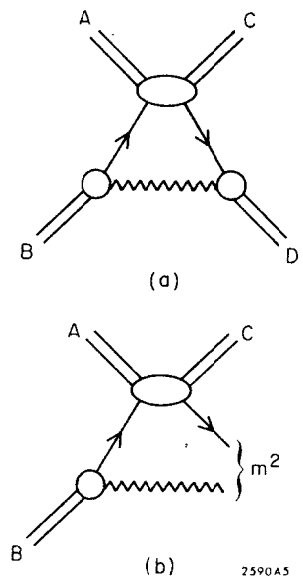

Figure 12

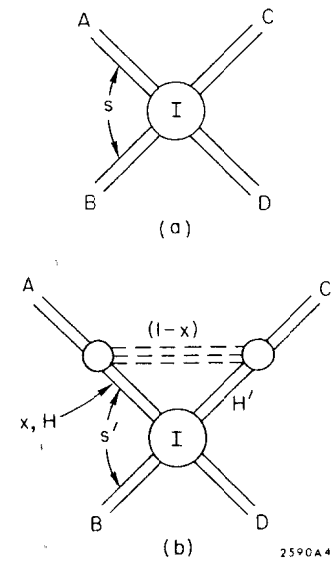

Figure 13

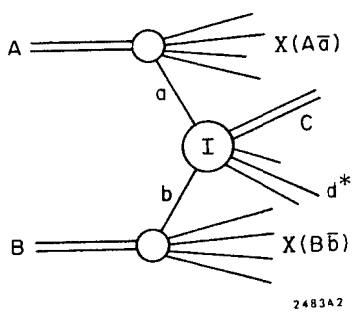

Figure 14

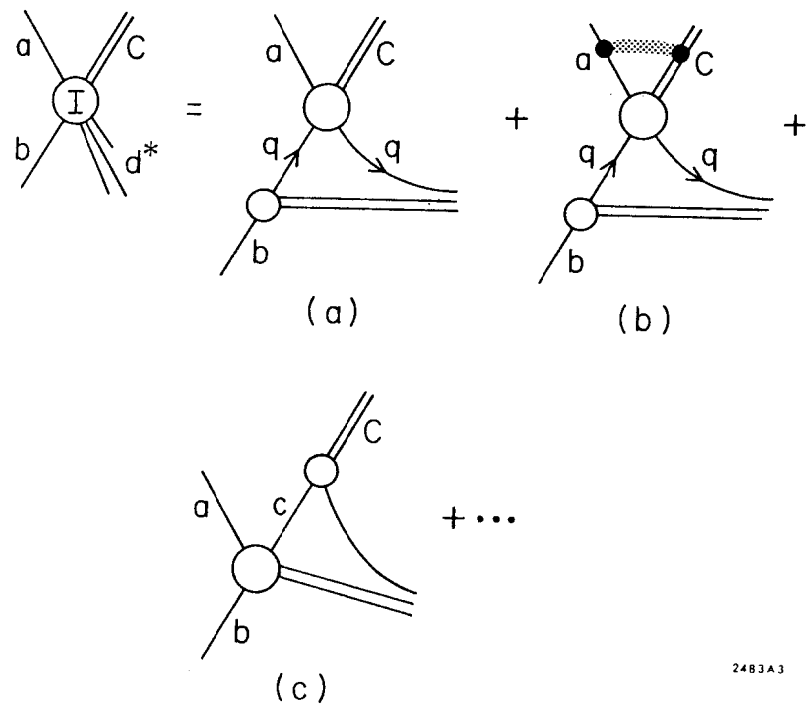

Figure 15

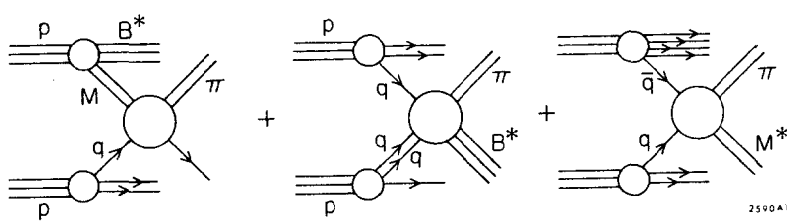

Figure 16

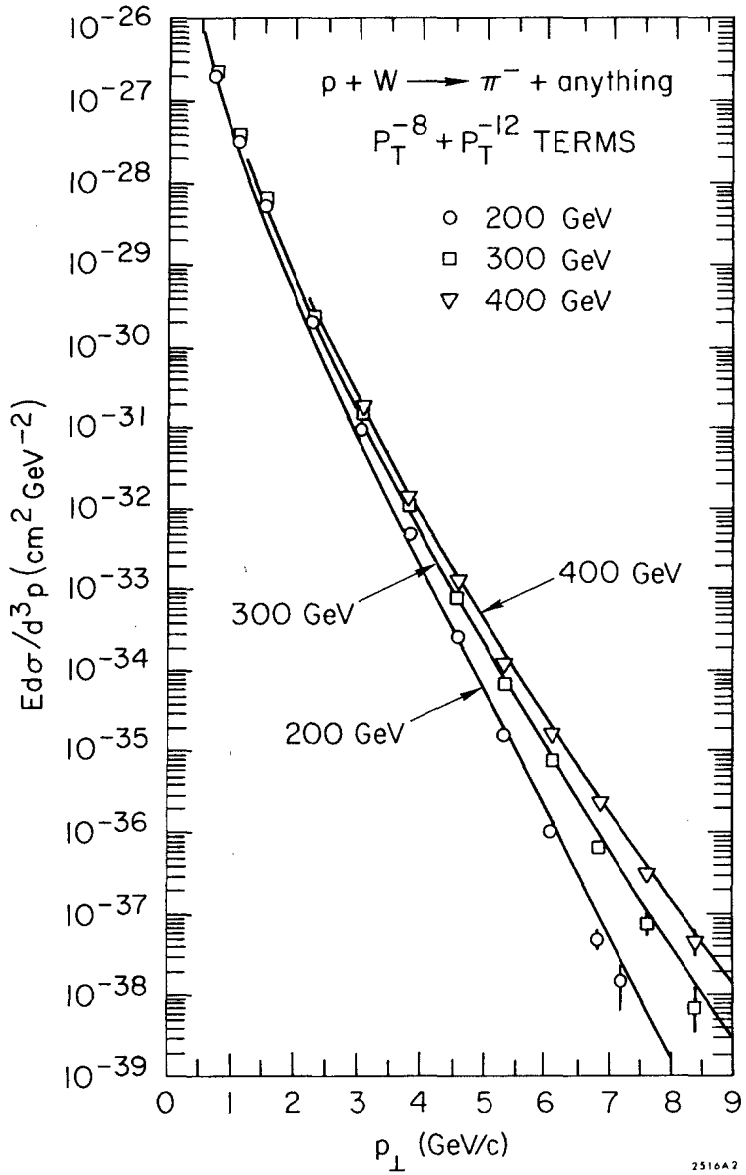

Figure 17

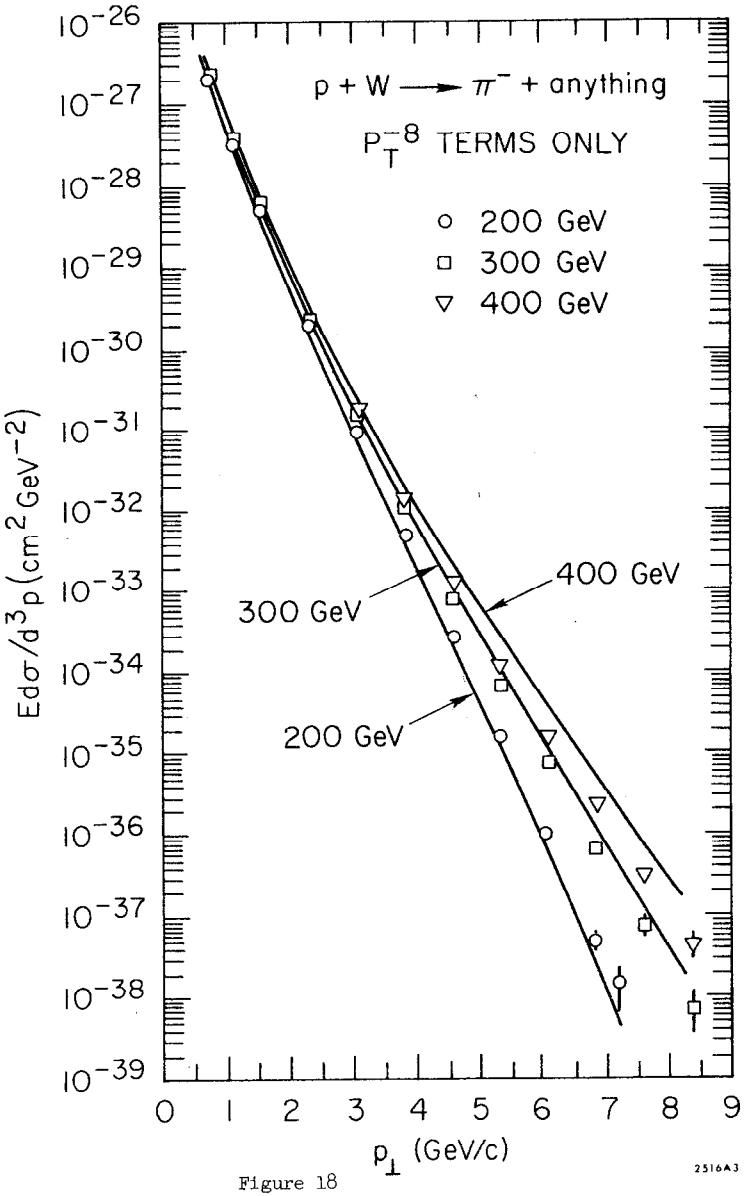

Figure 18

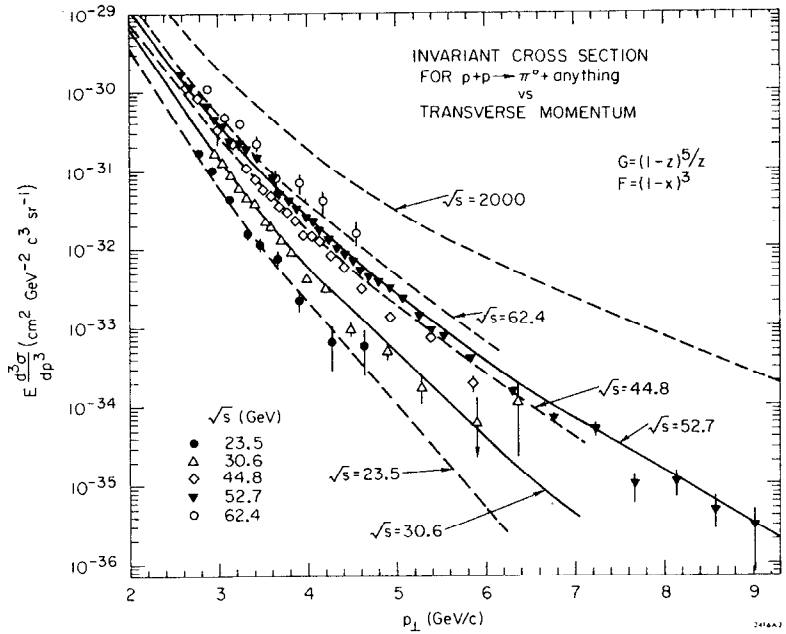

Figure 19

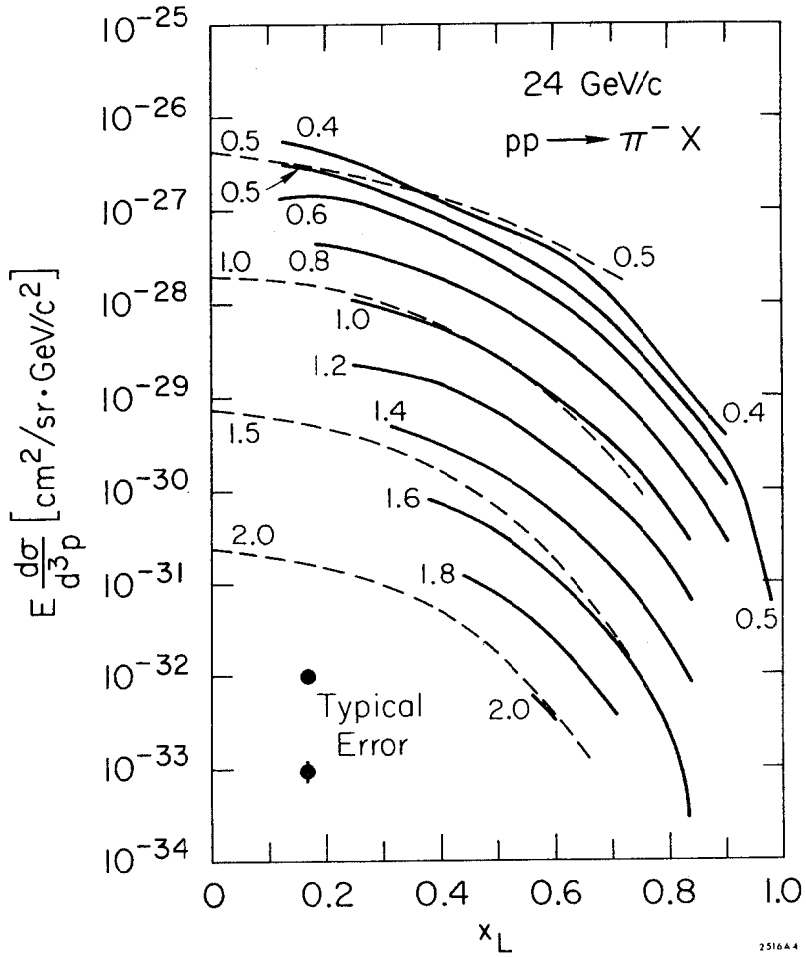

Figure 20

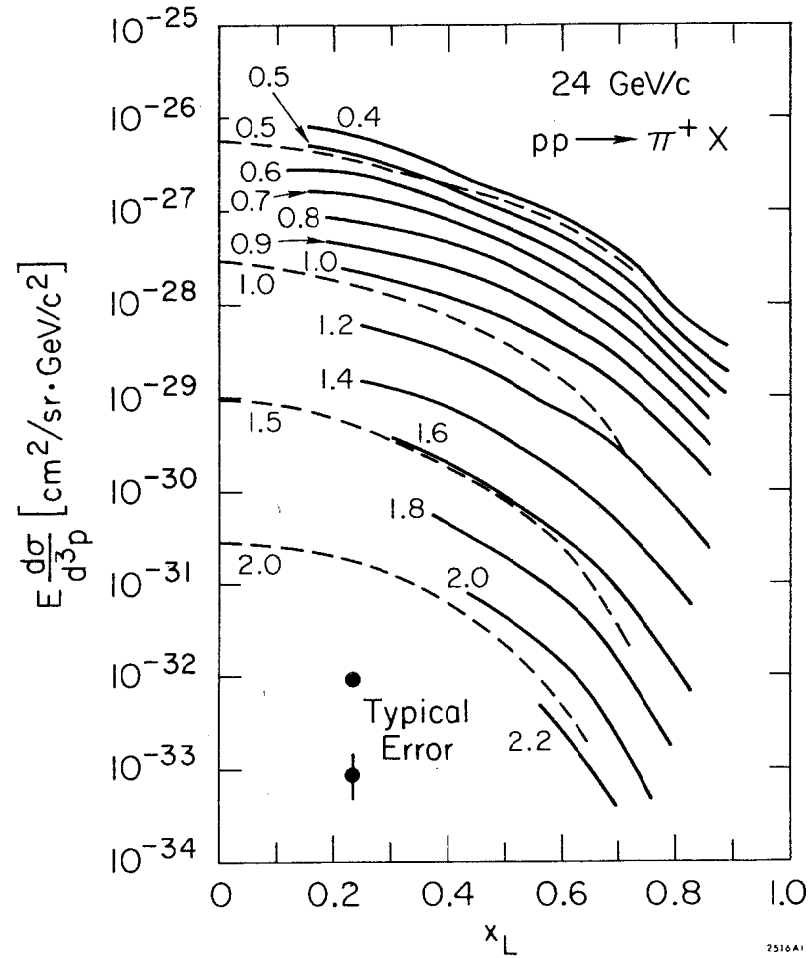

Figure 21

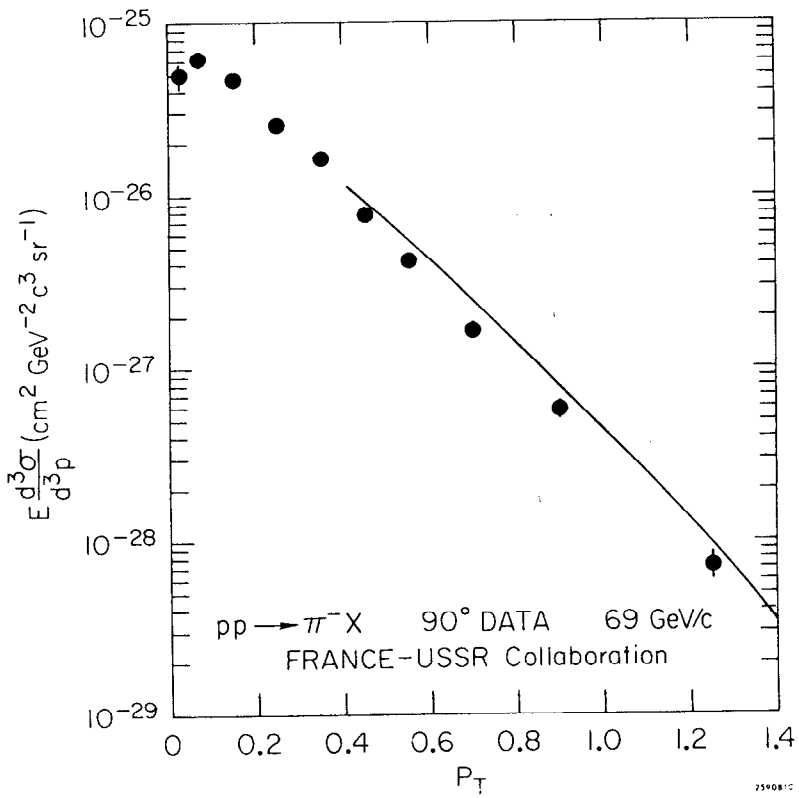

Figure 22

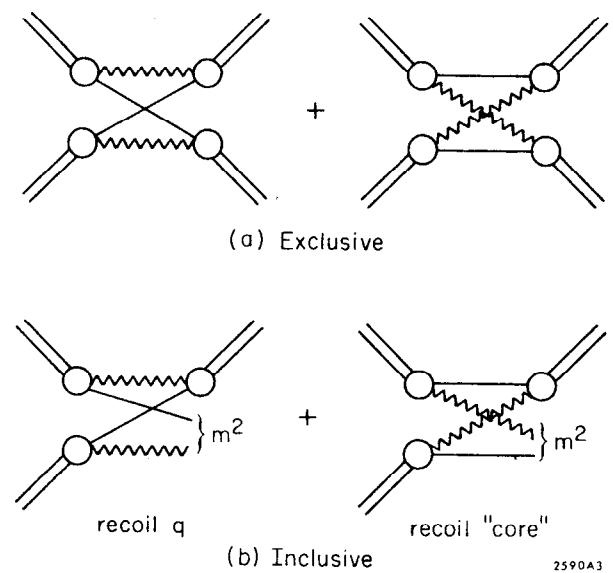

Figure 23

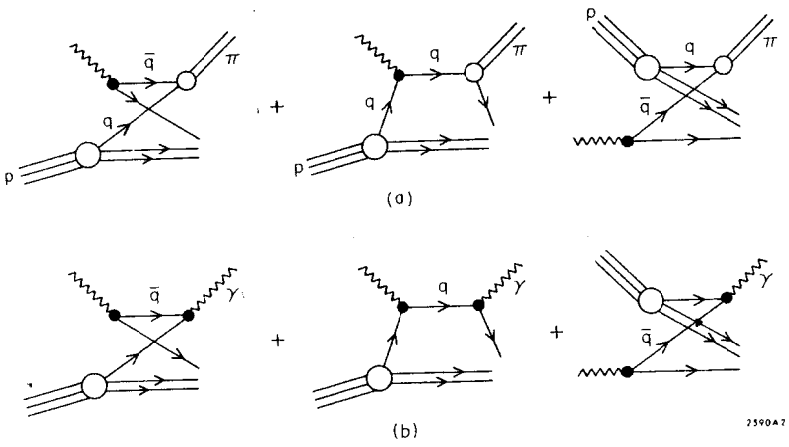

Figure 24